Jül-4325

Institut für Energieforschung (IEF)
Sicherheitsforschung und Reaktortechnik (IEF-6)

TOTMOS: An Integral Transport Code for Calculating Neutron Spectra and Multigroup Cross Sections

H. Brockmann

Mitglied der Helmholtz-Gemeinschaft

JÜLICH
FORSCHUNGSZENTRUM

TOTMOS: An Integral Transport Code for Calculating Neutron Spectra and Multigroup Cross Sections

H. Brockmann

Berichte des Forschungszentrums Jülich; 4325
ISSN 0944-2952
Institut für Energieforschung (IEF)
Sicherheitsforschung und Reaktortechnik (IEF-6)
Jül-4325

Vollständig frei verfügbar im Internet auf dem Jülicher Open Access Server (JUWEL)
unter http://www.fz-juelich.de/zb/juwel

Zu beziehen durch: Forschungszentrum Jülich GmbH · Zentralbibliothek, Verlag
D-52425 Jülich · Bundesrepublik Deutschland
☎ 02461 61-5220 · Telefax: 02461 61-6103 · e-mail: zb-publikation@fz-juelich.de

TOTMOS: An Integral Transport Code for Calculating Neutron Spectra and Multigroup Cross Sections

H. Brockmann

ABSTRACT

This report describes the TOTMOS code, which calculates the scalar neutron spectrum in a reactor cell as a function of the position by the collision probability method. One-dimensional cylindrical or spherical geometries can be treated. The neutron spectrum is used to compute cell-weighted cross sections, which can be used in gross reactor calculations. Furthermore, "equivalent" cross sections are calculated, which are employed to study the efficiency of absorber rods in a reactor on the basis of the diffusion theory.

CONTENTS

1 INTRODUCTION

The present report describes the TOTMOS code, which solves the integral neutron transport equation in one-dimensional cylindrical and spherical geometry by the method of collision probabilities.[1] The TOTMOS code is used as a neutron spectrum code in order to generate cell-weighted group cross sections for gross reactor calculations and to determine "equivalent" cross sections[2–4] for absorber rod calculations. The method of equivalent cross sections represents one of the methods which makes it possible to study the efficiency of absorber rods in a reactor by of the diffusion theory.

The TOTMOS code emerged in different stages of development from the THERMOS code,[5] which was written to calculate thermal neutron spectra in one-dimensional slab and cylindrical reactor lattices and to generate thermal broad-group cross sections. The first major change made in comparison to the original THERMOS code was the extension of the solution method to include the whole energy range as required for reactor calculations.[6] A further modification was that the TOTMOS code no longer uses the velocity as a variable but the energy. This makes it possible to use cross section data generated by the common multigroup cross section processing codes without major additional conversions. The THERMOS code solves a fixed source problem, where the sources for the thermal energy range are the inscatter processes from the epithermal energy range into the thermal range. The calculation of the neutron spectrum in the TOTMOS code for both fast and thermal energies therefore made it necessary to solve a different type of transport equation and the code was changed so that it solves an eigenvalue problem.

In a second step, the original integration method used in the THERMOS code for calculating the collision probabilities was replaced by a new and more efficient integration technique, which was first developed and realized for cylindrical geometry.[7] In this technique, the determination of the collision probabilities is reduced to the calculation of escape probabilities and the escape probabilities are determined in such a way that the integration over the source volume is coupled to the possible directions of flight, in which the source particles intersect with the system under consideration. The treatment of slab lattices was

abandoned in connection with the transition to the new integration technique. Furthermore, the option for the reflecting boundary condition was omitted due to problems connected with this boundary condition in cell calculations.[8] Instead, the possibility was incorporated into the TOTMOS code of using a white or albedo boundary condition at the outer surface of the system under consideration in addition to the vacuum boundary condition.[8,9] In a further step, it was shown that the new integration method for calculating the collision probabilities can also be extended without major changes to one-dimensional spherical geometries.[10]

Additionally, the TOTMOS code was revised with respect to number of other aspects.[11] Thus, all data fields used in the code are variably dimensioned and held in a container array, which makes it possible to adapt the storage requirements in a TOTMOS run to the specific problem of interest. The editing of the results, as for example, the fluxes and the balance tables, was modified in order to improve the readability of the output. Furthermore, the programming in the calculation of cel- weighted cross sections was totally revised. In this context, the TOTMOS code was modified so as to treat in two subsequent calculations double-heterogeneous systems, as they occur in high temperature reactors. Here, the nuclear fuel is used in the form of coated particles, which are embedded either in spherical fuel elements or in the rods of block-shaped fuel elements.[12] Finally, the option was incorporated into the TOTMOS code of computing equivalent cross sections for the absorber rod calculations.[a] During these revisions, the new name TOTMOS was also chosen for the code in order to indicate its descent from the THERMOS code and to describe the fact that the code treats the total energy range of interest in reactor physics.[13]

After this introduction in Section 1, a derivation of the integral transport equation is given in Section 2. This form of the transport equation is the basis and starting point of the collision probability method used in the TOTMOS code. The method of collision probabilities for solving the integral transport equation is described in Section 3. Furthermore, the properties of the collision probabilities, as for example the reciprocity relation, are discussed. The

[a]It should be mentioned here that the possibility was also incorporated into the TOTMOS code of performing a burn-up calculation in order to determine the depletion of the boron-10 isotope in a zone containing borated material. This fact is not further discussed in this report and is only explicitly addressed in the input description for the TOTMOS code.

transport coefficients are connected to the collision probabilities and are defined as the volume average of the transport kernel of the integral transport equation over a source region and as an integral over a target region. If the total cross section in a target region is zero recourse has to be taken to the use of the transport coefficients.

It is shown in Section 4 that the calculation of the collision probabilities can be reduced to the calculation of escape probabilities. This procedure can be applied to most spatial transfers which occur in a practical problem. Section 5 deals with the computation of the escape and collision probabilities and, if needed, with the explicit calculation of the transport coefficients. The determination of the escape probabilities requires the solution of a five fold integral. It is explained that four integrations can be performed analytically such that the problem is reduced to the evaluation of a one-dimensional integral, which is solved numerically. Depending on the properties of the source and target regions six case distinctions have to be made in the calculation of the collision probabilities and of the transport coefficients, which are described in Section 5 as well. It is furthermore explained how the concept of the albedo boundary condition can be incorporated into the collision probability method. It has to be ensured that numerical inaccuracies in the calculation of the escape or collision probabilities do not have a detrimental influence on the particle balance. For this reason the collision probabilities and the escape probability for leaving the system are normalized in an appropriate manner. The procedure in the normalization process is described. Furthermore, the sequence of the calculations of the collision probabilities by the use of the reciprocity relations for the collision probabilities and for the transport coefficients is explained.

The integral transport equation in the form of the collision equations is solved by the application of the power iteration method and by the use of source iterations. The power iteration method is combined with additional numerical techniques in order to accelerate the convergence. These are the normalization (or scaling), the over-relaxation, and the extrapolation, which represents a special form of over-relaxation. The iteration techniques used are discussed in Section 6.

The cross section data employed in the TOTMOS code are described in Section 7. The main portion of the data required in a TOTMOS run are taken from an external library,

which has the format of the cross section library used in the MUPO code.[14] For nuclei, for which no chemical binding effects need to be considered, the free-gas model[1] may be used in the TOTMOS code in order to determine the thermal scattering cross sections and thermal scattering kernels. Here, the Brown and St. John form of the free-gas model is employed.[15] The scattering kernels are averaged by a weighting function in order to calculate the group-to-group transfer cross sections for the free-gas model. The weighting function used in the TOTMOS code is based on the Westcott formalism,[16] which is also presented in Section 7. The format of the MUPO cross library is described in Section 8.

Section 9 deals with the computation of the cell-weighted cross sections by the TOTMOS code. The method used for the determination of the equivalent cross sections for the absorber rod calculations is explained in Section 10. Section 11 presents a short description of all the subroutines of the TOTMOS code.

Section 12 gives the input instructions for the TOTMOS code. The input data required to run a problem with the TOTMOS code are listed and a description of each input item is given. Furthermore, the logical units are needed for the input and output, are specified. A list of the literature used for preparing the present report is compiled in Section 13.

The following nomenclature is used. A zone is defined as a spatial region which exhibits the same material properties and may be subdivided into further spatial intervals. A lower case sigma (σ) is employed to represent the microscopic cross sections and the capital sigma (Σ) is used for the macroscopic cross sections. A lower index is utilized in order to specify the reaction type of a specific cross section. If additional indices are required, in order to specify for example the spatial interval or the energy group for which the cross section is defined, the lower index for the reaction type is changed into an upper index. The terms scattering matrices and group-to-group transfer cross sections are used synonymously. In the section describing the iteration methods used in the TOTMOS code, the macroscopic scattering matrices are also denoted by the capital letter P, in order to simplify the notation in the equations used there. The symbol Φ is employed for the angular flux and for the total flux. The distinction between the two quantities is indicated by the arguments. Although other arrangements are conceivable, the common procedure is used to give the geometric dimensions in centimeters, the dimensions of the cross sections in barns per atom and the

atomic number densities in atoms per barn and centimeter. The dimension of the scalar group flux is then neutrons per cm^2 and source neutron and that of the zone integrated group flux is cm per source neutron. The neutron energies are given in electron volt. The dimensions of the other quantities used in the TOTMOS code may be deduced from these definitions. It should also be mentioned that the notation used in this report is different from that employed in the TOTMOS code.

The author would like to thank Dr. W. Scherer, formerly at the Institute of Energy Research of Forschungszentrum Jülich, for many helpful discussions and assistance in clarifing for the author numerous areas addressed in the TOTMOS code. He is also indebted to Ms A. Kuhr of the same institute for her help in the preparation of the figures used in this report.

2 THE INTEGRAL TRANSPORT EQUATION

The neutron population in a nuclear system is commonly described by the angular flux

$$\Phi(\mathbf{r}, E, \mathbf{\Omega}) = v\, n(\mathbf{r}, E, \mathbf{\Omega})\,, \tag{1}$$

where $n(\mathbf{r}, E, \mathbf{\Omega})dV\,dE\,d\mathbf{\Omega}$ is the average number of neutrons in the volume element dV about the space point $\mathbf{r}$, in the energy interval dE about the energy E and in the solid angle element $d\mathbf{\Omega}$ about the direction $\mathbf{\Omega}$ and v is the absolute value of the neutron velocity. The angular flux $\Phi(\mathbf{r}, E, \mathbf{\Omega})$ can be determined by the time-independent neutron transport equation[1,17]

$$\mathbf{\Omega}\,\nabla\Phi(\mathbf{r}, E, \mathbf{\Omega}) + \Sigma_t(\mathbf{r}, E)\,\Phi(\mathbf{r}, E, \mathbf{\Omega}) = Q(\mathbf{r}, E, \mathbf{\Omega})\,, \tag{2}$$

which is a balance equation for the number of neutrons in the generalized volume element $dV\,dE\,d\mathbf{\Omega}$. The right side of Eq. (2) gives the neutron sources and the left side the neutron losses in the volume element. Furthermore, $\Sigma_t(\mathbf{r}, E)$ is the total cross section at the position $\mathbf{r}$ and at the energy E. The losses are absorption reactions, scattering processes, which remove the neutrons from the interval dE about E, and the neutron leakage out of the system under consideration. The neutron sources considered in the following are the scattering processes and the fission reactions. The total source density $Q(\mathbf{r}, E, \mathbf{\Omega})$ may then be written in the form

$$Q(\mathbf{r}, E, \mathbf{\Omega}) = S(\mathbf{r}, E, \mathbf{\Omega}) + F(\mathbf{r}, E, \mathbf{\Omega})\,, \tag{3}$$

where $S(\mathbf{r}, E, \mathbf{\Omega})$ is the neutron source density due to scattering processes and $F(\mathbf{r}, E, \mathbf{\Omega})$ the fission source density. The source density due to scattering may be written in the form

$$S(\mathbf{r}, E, \mathbf{\Omega}) = \int_{E'}\int_{\mathbf{\Omega}'} \Sigma_s(\mathbf{r}, E', \mathbf{\Omega}' \to E, \mathbf{\Omega})\,\Phi(\mathbf{r}, E', \mathbf{\Omega}')\,dE'd\mathbf{\Omega}' \tag{4}$$

where $\Sigma_s(\mathbf{r}, E', \mathbf{\Omega}' \to E, \mathbf{\Omega})$ is the transfer cross section, which describes how the energy and the direction of a neutron are changed (sich ändern) during a scattering event. The term $S(\mathbf{r}, E, \mathbf{\Omega})dV\,dE\,d\mathbf{\Omega}$ gives the number of neutrons in dV which emerge in the energy interval dE about E due to scattering processes from all other energies E' and in the solid angle element $d\mathbf{\Omega}$ about $\mathbf{\Omega}$ from all other directions $\mathbf{\Omega}'$.

In the calculation of the fission source density, it is a good approximation - also used in the TOTMOS code - to assume that the energy of the fission neutrons is independent of the incident neutron energy and that the emission of the fission neutrons is isotropic in the laboratory system. Thus, the fission source does not depend on the direction $\mathbf{\Omega}$ and may be written in the form

$$F(\mathbf{r}, E, \mathbf{\Omega}) = \frac{1}{4\pi}\chi(E) \int_{E'} \int_{\mathbf{\Omega}'} \nu(E')\Sigma_f(\mathbf{r}, E')\, \Phi(\mathbf{r}, E', \mathbf{\Omega}')\, dE' d\mathbf{\Omega}'\,, \tag{5}$$

where $\Sigma_f(\mathbf{r}, E)$ is the fission cross section, $\nu(E)$ the average number of neutrons emitted in a fission process, and $\chi(E)$ is the energy distribution of the fission neutrons, which is normalized to unity.

The transfer cross section $\Sigma_s(\mathbf{r}, E', \mathbf{\Omega}' \rightarrow E, \mathbf{\Omega})$ only depends explicitly on the directions of flight before and after scattering in special cases, when for example the medium in which the particle transport is studied is moving or consists of a single crystal. In most practical applications, the transfer cross section is a function of the cosine of the scattering angle in the laboratory system $\mu_L = \mathbf{\Omega}' \cdot \mathbf{\Omega}$, i.e.

$$\Sigma_s(\mathbf{r}, E', \mathbf{\Omega}' \rightarrow E, \mathbf{\Omega}) = \Sigma_s(\mathbf{r}, E' \rightarrow E, \mathbf{\Omega}' \cdot \mathbf{\Omega})\,. \tag{6}$$

Eq. (2) is an integro-differential equation. The method of collision probabilities is based on the integral form of the transport equation and Eq. (2) is therefore first converted into the required form using the method of characteristics. This method solves the transport equation along the direction of flight $\mathbf{\Omega}$. For this purpose, the leakage term $\mathbf{\Omega}\,\nabla\Phi$ is converted into a different form. In a Cartesian coordinate system the leakage term is given by

$$\mathbf{\Omega}\,\nabla\Phi = (\Omega_x \frac{\partial}{\partial x} + \Omega_y \frac{\partial}{\partial y} + \Omega_z \frac{\partial}{\partial z})\,\Phi\,. \tag{7}$$

If s denotes the space variable along the direction of flight $\mathbf{\Omega}$ (see Fig. 1), the total derivative of the angular flux is given by

$$\frac{d\Phi}{ds} = \frac{\partial\Phi}{\partial x}\frac{dx}{ds} + \frac{\partial\Phi}{\partial y}\frac{dy}{ds} + \frac{\partial\Phi}{\partial z}\frac{dz}{ds}\,. \tag{8}$$

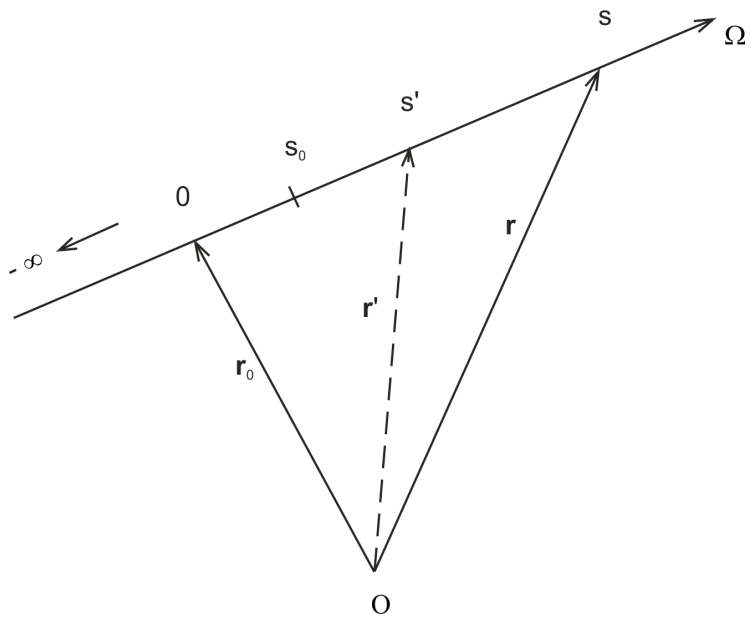

Fig. 1: Spatial coordinate along the direction of flight $\mathbf{\Omega}$.

A comparison of the Eqs.(7) and (8) gives the relations

$$\begin{aligned} \frac{dx}{ds} &= \Omega_x\,, & x &= x_0 + s\Omega_x \\ \frac{dy}{ds} &= \Omega_y\,, & y &= y_0 + s\Omega_y \\ \frac{dz}{ds} &= \Omega_z\,, & z &= z_0 + s\Omega_z\,, \end{aligned} \tag{9}$$

which can be written in the vector representation as

$$\mathbf{r} = \mathbf{r}_0 + s\,\mathbf{\Omega}\,. \tag{10}$$

Thus, the transport equation may be represented by

$$\frac{d}{ds}\Phi(\mathbf{r}_0 + s\mathbf{\Omega}, E, \mathbf{\Omega}) + \Sigma_t(\mathbf{r}_0 + s\mathbf{\Omega}, E)\,\Phi(\mathbf{r}_0 + s\mathbf{\Omega}, E, \mathbf{\Omega}) = Q(\mathbf{r}_0 + s\mathbf{\Omega}, E, \mathbf{\Omega}) \tag{11}$$

or abbreviated by

$$\frac{d\Phi}{ds} = -a(s)\Phi(s) + Q(s)\,, \tag{12}$$

where $a(s)$ is the abbreviation for the total cross section. If it is assumed that the function $\Phi(s)$ in the source term $Q(s)$ is known, an ordinary differential equation of first order is obtained, which can be solved by a variation of the constant. The solution of the homogeneous

equation is

$$\Phi(s) = c \, \exp\left[- \int_{s_0}^{s} a(s') ds' \right] . \tag{13}$$

The complete solution is the sum of the inhomogeneous and of the homogeneous solution, i.e.

$$\Phi(s) = \int_{s_0}^{s} Q(s') \, \exp\left[- \int_{s'}^{s} a(s'') ds'' \right] ds' + c \, \exp\left[- \int_{s_0}^{s} a(s') ds' \right] \tag{14}$$

with $c = \Phi(s_0)$, where s_0 is an arbitrary point on the connection line of the points $\mathbf{r}'$ and $\mathbf{r}$. Thus

$$\Phi(s) = \int_{s_0}^{s} Q(s') \, \exp\left[- \int_{s'}^{s} a(s'') ds'' \right] ds' + \Phi(s_0) \, \exp\left[- \int_{s_0}^{s} a(s') ds' \right] . \tag{15}$$

If s_0 is set equal to s_B, the value of s at the boundary of the system under consideration, and if there is no incoming flux (this corresponds the vacuum or free-surface boundary condition), the solution becomes, because of $\Phi(s_B) = 0$,

$$\Phi(s) = \int_{s_B}^{s} Q(s') \, \exp\left[- \int_{s'}^{s} a(s'') ds'' \right] ds' . \tag{16}$$

If there is an incoming flux, the latter can be treated as a surface source with free-surface boundary conditions.[17] In the literature, the lower integral limit is commonly extended to minus infinity. With $s_B \to -\infty$, Eq. (16) goes over into

$$\Phi(s) = \int_{-\infty}^{s} Q(s') \, \exp\left[- \int_{s'}^{s} a(s'') ds'' \right] ds' \tag{17}$$

or into

$$\Phi(\mathbf{r}_0 + s\mathbf{\Omega}, E, \mathbf{\Omega}) = \int_{-\infty}^{s} Q(\mathbf{r}_0 + s'\mathbf{\Omega}, E, \mathbf{\Omega}) \, \exp\left[- \int_{s'}^{s} \Sigma_t(\mathbf{r}_0 - s''\mathbf{\Omega}, E) \, ds'' \right] ds' . \tag{18}$$

The vector $\mathbf{r}_0$ on the right side of Eq. (18) is now replaced by $\mathbf{r} - s\mathbf{\Omega}$. Furthermore, the variables s' and s'' are transformed in a such way that they are no longer counted from the point $\mathbf{r}_0$ but from the target point $\mathbf{r}$ (see also Fig. 1). Thus, the following result is obtained

$$\Phi(\mathbf{r}, E, \mathbf{\Omega}) = \int_{0}^{\infty} Q(\mathbf{r} - s'\mathbf{\Omega}, E, \mathbf{\Omega}) \, \exp\left[- \int_{0}^{s'} \Sigma_t(\mathbf{r} - s''\mathbf{\Omega}, E) \, ds'' \right] ds' . \tag{19}$$

The integral term, which appears in the exponential function of Eq. (19), is the optical path length

$$\tau(\mathbf{r}', \mathbf{r}) = \int_{0}^{s'} \Sigma_t(\mathbf{r} - s''\mathbf{\Omega}, E) \, ds'' \tag{20}$$

between the source point $\mathbf{r}'$ and the target point $\mathbf{r}$. The optical path length is a measure of the attenuation of the neutrons during their flight through matter.

3 THE COLLISION PROBABILITY METHOD

In the following, the reactor cell to be analyzed is divided into a number, K, of spatial intervals. The volume of the kth interval ($k = 1, 2, \cdots, K$) is denoted by V_k. The total number of collisions in the interval k of a heterogeneous configuration due to neutrons in the energy interval dE about E is then obtained by multiplying the integral transport equation in Eq. (19) by $\Sigma_t(\mathbf{r}, E)$ and integrating the resulting equation over the volume V_k and over all directions $\mathbf{\Omega}$, i.e.

$$\int_{V_k}\int_{\mathbf{\Omega}} \Sigma_t(\mathbf{r}, E)\, \Phi(\mathbf{r}, E, \mathbf{\Omega}) dV d\mathbf{\Omega} dE$$
$$= \int_{V_k}\int_{\mathbf{\Omega}}\int_{s'} Q(\mathbf{r} - s'\mathbf{\Omega}, E, \mathbf{\Omega})\, \Sigma_t(\mathbf{r}, E)\, e^{-\tau(\mathbf{r}', \mathbf{r}, E)} ds' d\mathbf{\Omega} dV dE\,. \tag{21}$$

If the origin of the coordinate system is shifted into the detector point $\mathbf{r}$, it is seen that the integrations over s' and $\mathbf{\Omega}$ correspond to a volume integration using spherical polar coordinates, i.e.

$$dV' = s'^2 ds' d\mathbf{\Omega}$$

or

$$d\mathbf{\Omega}\, ds' = \frac{dV'}{s'^2} = \frac{dV'}{|\mathbf{r} - \mathbf{r}'|^2}\,.$$

Thus, Eq. (21) becomes

$$\int_{V_k}\int_{\mathbf{\Omega}} \Sigma_t(\mathbf{r}, E)\, \Phi(\mathbf{r}, E, \mathbf{\Omega}) dV d\mathbf{\Omega} = \int_{V_k}\int_{V'} Q(\mathbf{r}', E, \mathbf{\Omega})\, \Sigma_t(\mathbf{r}, E)\, \frac{e^{-\tau(\mathbf{r}', \mathbf{r}, E)}}{|\mathbf{r} - \mathbf{r}'|^2}\, dV' dV\,, \tag{22}$$

where the integration over $\mathbf{r}'$ is perfomed over the whole cell. Furthermore, the average flux density

$$\Phi_k(E) = \frac{1}{V_k}\int_{V_k}\int_{\mathbf{\Omega}} \Phi(\mathbf{r}, E, \mathbf{\Omega}) dV d\mathbf{\Omega} \tag{23}$$

and the average source density

$$Q_k(E) = \frac{1}{V_k}\int_{V_k}\int_{\mathbf{\Omega}} Q(\mathbf{r}, E, \mathbf{\Omega}) dV d\mathbf{\Omega}\,, \tag{24}$$

in the interval k are introduced. If the total cross section on left-hand side of Eq. (22) is additionally expressed by the flux averaged cross section $\Sigma_k^t(E)$, the collision equations may

be written in the form

$$\Sigma_k^t(E)\Phi_k(E)V_k = \sum_{k'=1}^{K} Q_{k'}(E)\, P_{k'k}(E)\, V_{k'}\,, \tag{25}$$

where

$$P_{k'k}(E) = \frac{1}{V_{k'}\, Q_{k'}(E)} \int_{V_k}\int_{V_{k'}} \Sigma_t(\mathbf{r}, E) Q(\mathbf{r}', E, \mathbf{\Omega})\, \frac{e^{-\tau(\mathbf{r}', \mathbf{r}, E)}}{|\mathbf{r}-\mathbf{r}'|^2}\, dV' dV \tag{26}$$

is the probability that a neutron is born in the interval k' due to a scattering or fission process and makes the next collision in the interval k. This can be seen if the coordinate system for the $\mathbf{r}$ integration is shifted into the source point $\mathbf{r}'$. The volume element dV may then be written as

$$dV = |\mathbf{r}-\mathbf{r}'|^2\; ds\, d\mathbf{\Omega}\,. \tag{27}$$

The term

$$\frac{Q(\mathbf{r}', E, \mathbf{\Omega})}{Q_{k'}(E)\, V_{k'}}\, dV' d\mathbf{\Omega}\, e^{-\tau(\mathbf{r}', \mathbf{r}, E)}$$

is the probability that a neutron is born due a scattering process or a fission reaction in the volume element dV' about $\mathbf{r}'$ and in the solid angle element $d\mathbf{\Omega}$ about the direction $\mathbf{\Omega}$ and reaches the space point $\mathbf{r}$ without collision. The term $\Sigma_t(\mathbf{r}, E)ds$ is the probability that the neutron makes the next collision in the interval ds about the point $\mathbf{r}$.

In order to calculate the collision probability in practical applications, a spatially constant (flat source approximation) and isotropic source density is assumed. In this case, the collision probability is given by

$$P_{k'k}(E) = \frac{1}{V_{k'}} \int_{V_k}\int_{V_{k'}} \Sigma_t(\mathbf{r}, E)\, \frac{e^{-\tau(\mathbf{r}', \mathbf{r}, E)}}{4\pi\, |\mathbf{r}-\mathbf{r}'|^2}\, dV' dV \tag{28}$$

and depends only on the spatial structure and the total cross sections of the configuration to be analyzed. In order to enable an analytical evaluation of the collision probability, it is furthermore assumed in the following that the total cross section in the interval k is constant. This is a justified assumption if a sufficiently fine spatial division of the reactor cell is chosen. Thus,

$$P_{k'k}(E) = \frac{\Sigma_k^t(E)}{V_{k'}} \int_{V_k}\int_{V_{k'}} \frac{e^{-\tau(\mathbf{r}', \mathbf{r}, E)}}{4\pi\, |\mathbf{r}-\mathbf{r}'|^2}\, dV' dV\,. \tag{29}$$

In order to simplify the notation, the energy variable is omitted in the following when its use is not required for understanding.

The quantity

$$T(\mathbf{r}', \mathbf{r}) = \frac{e^{-\tau(\mathbf{r}', \mathbf{r})}}{4\pi \left|\mathbf{r} - \mathbf{r}'\right|^2}\,, \tag{30}$$

which occurs under the integral for the collision probability, is called the transport kernel, for which the relation

$$T(\mathbf{r}', \mathbf{r}) = T(\mathbf{r}, \mathbf{r}') \tag{31}$$

holds. The transport kernel is the uncollided neutron flux at the position $\mathbf{r}$ due to an isotropic neutron source at the position $\mathbf{r}'$.

Due to the assumption that the total cross section in the interval k is constant, a reciprocity relation for the collision probabilities can be derived from Eq. (29), which is

$$\frac{V_{k'} P_{k'k}}{\Sigma_k^t} = \frac{V_k P_{kk'}}{\Sigma_{k'}^t} \tag{32}$$

or

$$V_{k'} \Sigma_{k'}^t P_{k'k} = V_k \Sigma_k^t P_{kk'}\,. \tag{33}$$

In addition to the collision probabilities, the transport coefficients are defined by

$$T_{k'k} = \frac{1}{V_k} \int_{V_k} \int_{V_{k'}} T(\mathbf{r}', \mathbf{r})\, dV' dV = \frac{1}{V_k} \int_{V_k} \int_{V_{k'}} \frac{e^{-\tau(\mathbf{r}', \mathbf{r})}}{4\pi \left|\mathbf{r} - \mathbf{r}'\right|^2}\, dV' dV\,. \tag{34}$$

are defined by. They have the property

$$T_{k'k} = \frac{V_{k'}}{V_k} T_{kk'} \tag{35}$$

and are related to the collision probabilities by the equation

$$T_{k'k} = \frac{V_{k'}}{V_k \Sigma_k^t}\, P_{k'k}\,. \tag{36}$$

If the total cross section in the target interval k is zero, the collision probability $P_{k'k}$ vanishes and one has to go back in this case to the transport coefficient $T_{k'k}$.

If the system under consideration has a conserving boundary condition, the equation

$$\sum_k V_k \Sigma_k^t T_{k'k} = 1 \tag{37}$$

must be fulfilled. This leads to the following statement of neutron conservation

$$\sum_{k=1}^{K} V_k \int_E \Sigma_k^a(E)\Phi_k(E)dE = \sum_{k=1}^{K} V_k \int_E F_k(E)dE\,, \tag{38}$$

which is obtained from Eq. (25) by the use of the normalization condition

$$\int_E \Sigma_k^s(E' \to E) = \Sigma_k^s(E')\,, \tag{39}$$

where $\Sigma_k^s(E')$ is the total scattering cross section in the interval k and at the energy E'. If a vacuum or an albedo boundary condition is used, the equation

$$\sum_{k=1}^{K} V_k \Sigma_k^t T_{k'k} = q_{k'}(E) \tag{40}$$

must hold, where $q_{k'}(E)$ is the first flight non-leakage probability. The statement of neutron conservation is then

$$\sum_{k=1}^{K} V_k \int_{E'} \Phi_k(E') \left[\Sigma_k^t(E') - \int_E q_k(E)\Sigma_k^s(E' \to E)dE\right] dE' = \sum_{k=1}^{K} V_k \int_E q_k(E)F_k(E)dE\,. \tag{41}$$

During the iteration process for solving the transport equation, extensive use of Eq. (38) or Eq. (41) is made in order to normalize the iterated flux $\Phi_k(E)$ and to conserve the global particle balance by this procedure.

4 REPRESENTATION OF THE COLLISION PROBABILITIES BY ESCAPE PROBABILITIES

In this section, it is shown that the calculation of the collision probabilities can be reduced to the calculation of escape probabilities. In the following derivation the positions at which the trajectory of a source particle starting at $\mathbf{r}'$ with the direction $\mathbf{\Omega}$ intersects the inner or the outer boundary of the target interval k are denoted by $\mathbf{r}_{k-1}$ and $\mathbf{r}_k$, respectively. The optical path length between the points $\mathbf{r}'$ and $\mathbf{r}$ may then be expressed by

$$\tau(\mathbf{r}', \mathbf{r}) = \tau(\mathbf{r}', \mathbf{r}_{k-1}) + \Sigma_k^t (s - s_{k-1}) \,, \tag{42}$$

where s_{k-1} is the geometrical path along the direction $\mathbf{\Omega}$ from the source point $\mathbf{r}'$ to the inner boundary of the interval k. If, furthermore, s_k denotes the geometric path length to the position $\mathbf{r}_k$ and s the length of the path to the point $\mathbf{r}$ in the interval k, it may be written

$$\begin{aligned}
\int_{V_k} dV \frac{e^{-\tau(\mathbf{r}', \mathbf{r})}}{|\mathbf{r} - \mathbf{r}'|^2} &= \int_{\mathbf{\Omega}} d\mathbf{\Omega} \int_{s_{k-1}}^{s_k} ds \, \exp - \left[\tau(\mathbf{r}', \mathbf{r}_{k-1}) + \Sigma_k^t (s - s_{k-1})\right] \\
&= \int_{\mathbf{\Omega}} d\mathbf{\Omega} \, e^{-\tau(\mathbf{r}', \mathbf{r}_{k-1})} \int_{s_{k-1}}^{s_k} ds \, \exp\left[-\Sigma_k^t (s - s_{k-1})\right] \\
&= -\frac{1}{\Sigma_k^t} \int_{\mathbf{\Omega}} d\mathbf{\Omega} \, e^{-\tau(\mathbf{r}', \mathbf{r}_{k-1})} \left\{\exp\left[-\Sigma_k^t (s_k - s_{k-1})\right] - 1\right\} \\
&= \frac{1}{\Sigma_k^t} \int_{\mathbf{\Omega}} d\mathbf{\Omega} \left[e^{-\tau(\mathbf{r}', \mathbf{r}_{k-1})} - e^{-\tau(\mathbf{r}', \mathbf{r}_k)}\right] .
\end{aligned} \tag{43}$$

If this result is inserted into Eq. (29), the following expression is obtained for the collision probability

$$\begin{aligned}
P_{k'k} &= \frac{1}{4\pi V_{k'}} \int_{V_{k'}} dV' \int_{\mathbf{\Omega}} d\mathbf{\Omega} \left[e^{-\tau(\mathbf{r}', \mathbf{r}_{k-1})} - e^{-\tau(\mathbf{r}', \mathbf{r}_k)}\right] \\
&= C_{k'k-1} - C_{k'k} \,,
\end{aligned} \tag{44}$$

where the quantity $C_{k'k}$ is defined by

$$C_{k'k} = \frac{1}{4\pi V_{k'}} \int_{V_{k'}} dV' \int_{\mathbf{\Omega}} d\mathbf{\Omega} \, e^{-\tau(\mathbf{r}', \mathbf{r}_k)} \,. \tag{45}$$

The meaning of $C_{k'k}$ can be seen from the following consideration. If the neutron source strength in the interval k' is constant and equal to unity, the expression

$$\frac{dV'}{V_{k'}} \frac{d\mathbf{\Omega}}{4\pi} e^{-\tau(\mathbf{r}', \mathbf{r}_k)}$$

is the probability that a neutron emerging in the volume element dV' about $\mathbf{r}'$ with directions in the solid angle element $d\mathbf{\Omega}$ about the direction $\mathbf{\Omega}$ reaches the outer boundary of the interval k without collision. Thus, $C_{k'k}$ is the probability that a particle emerging in interval k' leaves the interval k across the outer surface A_k without collision. This is the usual definition of the escape probability.

Eq. (44) can be interpreted as a balance equation. A neutron entering the interval k across the inner boundary A_{k-1} either makes a collision in k or leaves the interval across the outer boundary A_k without collision and this is finally the reason that the calculation of the collision probabilities can be reduced to the calculation of escape probabilities.

5 COMPUTATION OF THE ESCAPE AND COLLISION PROBABILITIES AND THE TRANSPORT COEFFICIENTS

5.1 General Considerations

In this section, the integrals in Eq. (45), which defines the escape probability $C_{k'k}$, are evaluated for one-dimensional cylindrical and spherical geometries. It is explained that four of the five integrations can be performed analytically. It is furthermore shown that the same procedure for calculating the escape probabilities can be used for both geometries and that essentially only the integrands of the remaining integral are different. These are the Bickley functions[18] in the case of the cylindrical geometry and the exponential function in the case of the spherical geometry. The procedure is first explained with the example of the cylindrical geometry. Depending on the spatial transition and on the total cross sections in the source interval or in the target interval, six case distinctions have to be made and are described. The collision probabilities $P_{k'k}$ can then be determined by the use of the calculated escape probabilities. If the total cross section in a target interval is zero, the transport coefficients $T_{k'k}$ have to be computed instead of the collision probabilities. The procedure for treating the spherical geometry is described subsequently.

5.2 Cylindrical Geometry

For cylindrical geometry, the coordinates of the position vector $\mathbf{r}$ are denoted by r, φ, z, where r is the projection of the vector $\mathbf{r}$ into the x-y plane, φ the polar angle, which is counted from the x-axis, and z is the usual axial coordinate (see Fig. 2). In curved geometries, the coordinates of the direction variable $\mathbf{\Omega}$ are given in a coordinate system which is connected to the spatial variable $\mathbf{r}$. This coordinate system is also shown in Fig. 2. It has its origin in position $\mathbf{r}$. The $\hat{\mathbf{e}}_z$-axis is parallel to the z-axis of the spatial coordinate system. The direction variable $\mathbf{\Omega}$ is described by the spherical polar coordinates θ and ω. The polar angle θ is counted from the $\hat{\mathbf{e}}_z$-axis. The azimuthal angle ω is the angle between the plane formed by the vectors $\hat{\mathbf{z}}$ and $\hat{\mathbf{r}}$ and the plane formed by the vectors $\hat{\mathbf{e}}_z$ and $\mathbf{\Omega}$, where $\hat{\mathbf{z}}$ is a unit

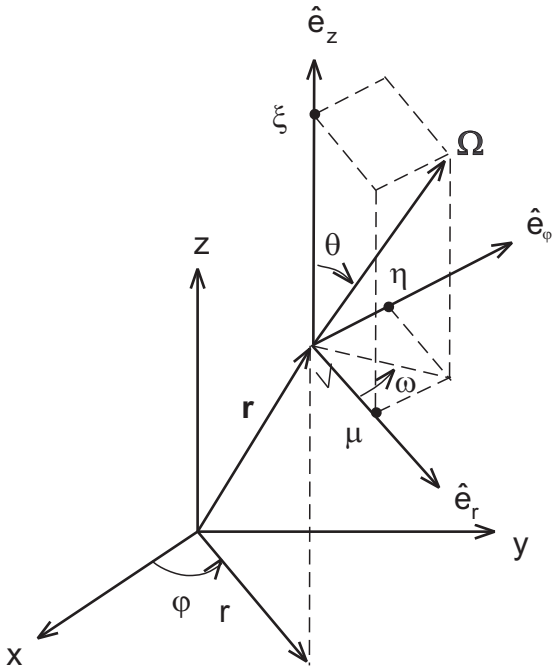

Fig. 2: Coordinates in cylindrical geometry. (The axis intercepts μ, η, ξ denote the Cartesian coordinates of the direction vector $\mathbf{\Omega}$).

vector in the z-direction. The solid angle element is then given by

$$d\mathbf{\Omega} = \sin\theta d\theta d\omega \,. \tag{46}$$

The infinitesimal source volume element dV' is given by

$$dV' = r' dr' d\varphi' dz' \,. \tag{47}$$

In order to evaluate the integrals in Eq. (45), it is convenient to express the optical path length $\tau(\mathbf{r}', \mathbf{r}_k)$ by the projection $t = \tau \sin\theta$ into x-y plane. The escape probability may then be written in the form

$$\begin{aligned} C_{k'k} &= \frac{1}{4\pi V_{k'}} \int_{V_{k'}} dV' \int_0^{\pi} d\theta \int_0^{2\pi} d\omega \, \sin\theta \, e^{-t/\sin\theta} \\ &= \frac{1}{4\pi V_{k'}} \, 2 \int_{V_{k'}} dV' \int_0^{\pi/2} d\theta \int_0^{2\pi} d\omega \, \sin\theta \, e^{-t/\sin\theta} \\ &= \frac{1}{2\pi V_{k'}} \int_{V_{k'}} dV' \int_0^{2\pi} d\omega \, Ki_2(t) \,, \end{aligned} \tag{48}$$

where $Ki_2(t)$ is the Bickley function of the order two. The Bickley functions are defined by

$$\begin{aligned} Ki_0(x) &= K_0(x) \\ Ki_n(x) &= \int_x^\infty dx'\, Ki_{n-1}(x') \quad \text{for } n \geq 1\,, \end{aligned} \tag{49}$$

where $K_0(x)$ is the modified Bessel function of the order zero.[18] The Bickley functions may be written in the form

$$Ki_n(x) = \int_0^{\pi/2} d\theta\, \sin^{n-1}\theta\, e^{-x/\sin\theta} \quad \text{for } n \geq 1\,. \tag{50}$$

For reasons of symmetry, the integration over the polar angle θ only needs to be performed explicitly over the range $0 \leq \theta \leq \pi/2$. Since the integrand in Eq. (48) does not depend on the source variable z', the cylinder height cancels out in the expression for the escape probability. Thus, the volumes $V_{k'}$ of the intervals k' (as the volumes V_k) are to be understood in cylindrical geometry in the sense that they are given for a unit height.

Fig. 3 shows the projections of the flight paths from the position $\mathbf{r}'$ in the source interval k' to the outer boundary of the interval k for different azimuthal angles ω. The projections of the optical path lengths may be expressed in the cylindrical coordinates by

$$t = t(r', \omega) = \Sigma_{k'}^t \left[\sqrt{r_{k'}^2 - (r' \sin\omega)^2} - r' \cos\omega\right] + t_{k'k}^*\,, \tag{51}$$

where $t_{k'k}^*$ is the optical path length from the outer boundary of the interval k' to the outer boundary of the interval k along the flight path belonging to ω. Since the possible trajectories do not depend on the angle φ', the integration over this variable can be performed, which gives a factor 2π. The escape probability $C_{k'k}$ can then in principle be determined by integration over the spatial variables r' and the azimuthal angle ω. It turns out, however, that it is convenient in practice not to use r' and ω as integration variables but to perform the spatial integration along the trajectories of the neutrons. The possible trajectories shown in Fig. 3 may be represented as parallels to the x-axis at different distances y in the x-y coordinate system and the outstanding integration over r' and ω is replaced by an integration along the parallels to the x-axis in the source interval k' (see Fig. 4).

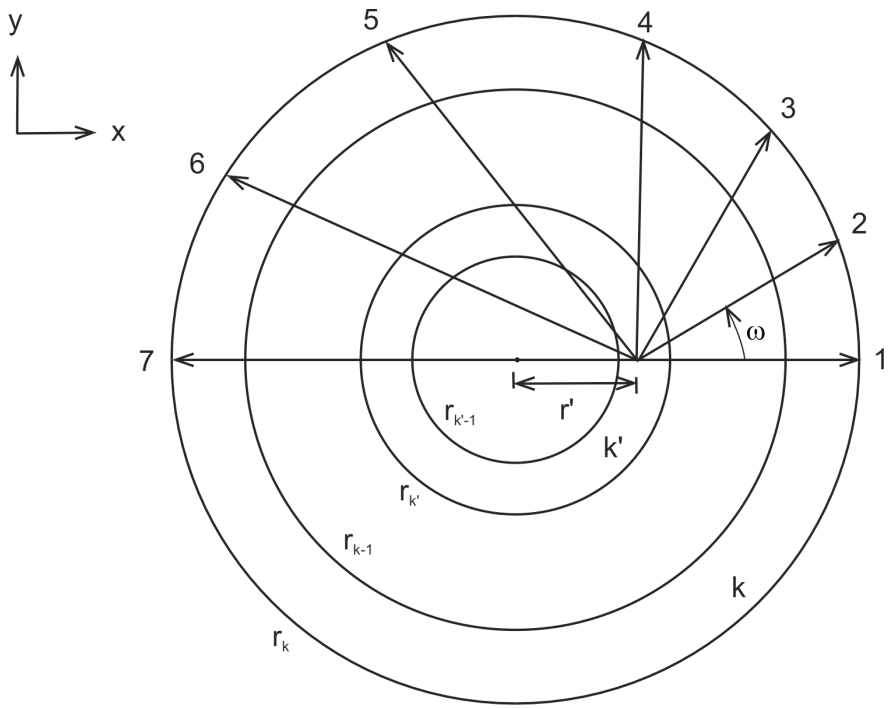

Fig. 3: Trajectories for different azimuthal angles ω.

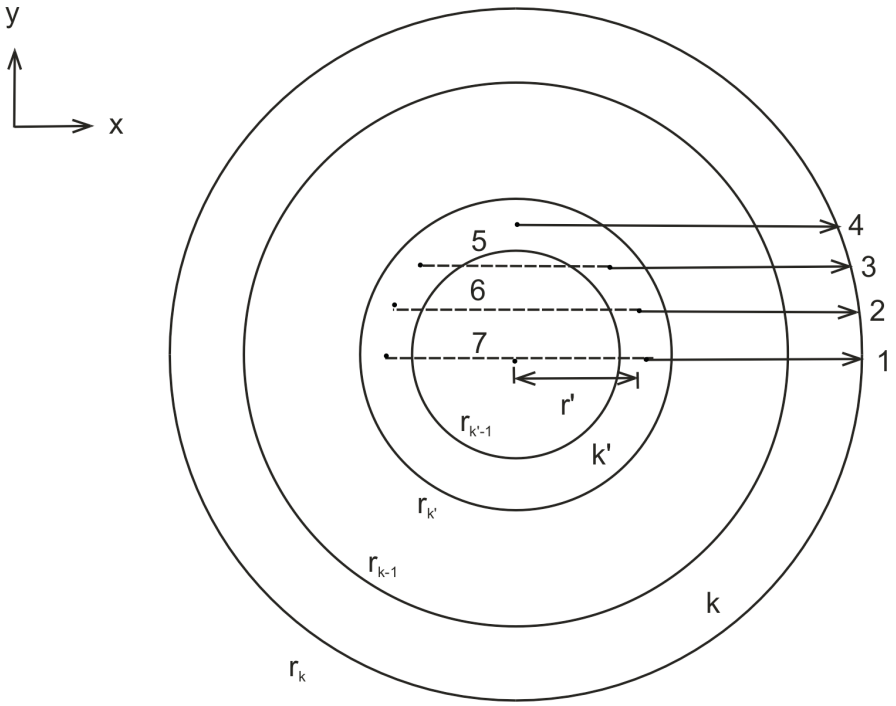

Fig. 4: Representation of the trajectories as parallels.

The procedure is realized by the variable transformations

$$\begin{aligned} x &= r' \cos\omega - r_{k'} \cos\omega_{k'} \\ y &= r' \sin\omega \end{aligned} \tag{52}$$

with

$$r' dr' d\omega = dx dy \,. \tag{53}$$

where $\omega_{k'}$ is the azimuthal angle of $\mathbf{\Omega}$ at the position where the flight path intersects the outer boundary of the interval k'. The optical path length t in Eq. (51) is given in the new coordinates by

$$t = t(x, y) = \Sigma_{k'}^{t} \left[a(y) - x \right] + t_{k'k}^{*} \,, \tag{54}$$

where $a(y)$ is the length of the chord or of a section of the chord which runs parallel to the x-axis at a distance y through the circle of the radius $r_{k'}$ or a circular ring with the outer radius $r_{k'}$, respectively (see Fig. 5). The variable x is counted from the intersection point of the parallel with the outer boundary of the interval k' in the second quadrant.

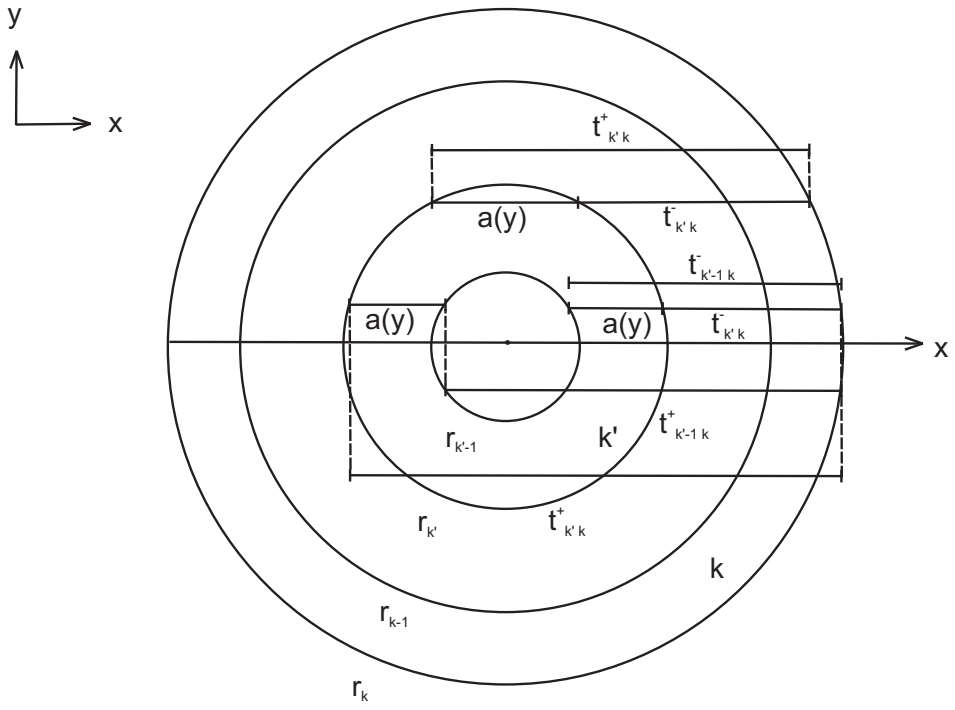

Fig. 5: Optical path lengths in the integration.

In order to show the further procedure for computing the escape probability exemplarily, the special case is considered in the following in which the source interval k' is the innermost interval. The collision probability $C_{k'k}$ may then be written in the form

$$C_{k'k} = \frac{1}{V_{k'}} \int_{-r_{k'}}^{r_{k'}} dy \int_0^{a(y)} dx \, Ki_2\{\Sigma_{k'}^t \, [a(y) - x] + t_{k'k}^*\} \, . \tag{55}$$

For reasons of symmetry, it is sufficient to perform the integration over y for $y \geq 0$ only. It is furthermore convenient to make the variable transformation $x' = \Sigma_{k'}^t x$. If the variable x' is subsequently again denoted by x and if the section $a(y)$ is also given in the following in mean free paths, Eq. (55) may be written as

$$C_{k'k} = \frac{2}{\Sigma_{k'}^t V_{k'}} \int_0^{r_{k'}} dy \int_0^{a(y)} dx \, Ki_2[\, a(y) - x + t_{k'k}^*] \, . \tag{56}$$

The derivative of the second expression in Eq. (49) with respect to x gives the relation

$$Ki_{n-1}(x) = -\frac{d}{dx} Ki_n(x) \quad \text{for } n \geq 1 \tag{57}$$

which allows the integration over x to be performed in Eq. (56). Thus

$$C_{k'k} = \frac{2}{\Sigma_{k'}^t V_{k'}} \int_0^{r_{k'}} dy \, \{Ki_3(t_{k'k}^*) - Ki_3[\, a(y) + t_{k'k}^*]\} \, . \tag{58}$$

In the following, the six case distinctions are discussed which have to be considered in the computation of the collision probabilities and the transport coefficients in practice. In the resulting expressions, the optical path lengths $t_{k'k}^-$, $t_{k'-1\,k}^-$, $t_{k'k}^+$, and $t_{k'-1\,k}^+$ occur, which are illustrated in Fig. 5. The length $t_{k'k}^-$ may be expressed by

$$t_{k'k}^- = \sum_{i=k'+1}^{k} x_i(y) \Sigma_i^t \, , \tag{59}$$

where $x_i(y)$ is the geometrical path length in the interval i in the first quadrant, and the length $t_{k'k}^+$ by

$$t_{k'k}^+ = t_{k'k}^- + 2 \sum_{i=1}^{k} x_i(y) \Sigma_i^t \, , \tag{60}$$

where $x_i(y) = 0$ for $y \geq r_i$. The collision probabilities and transport coefficients are calculated explicitly only for $k' \leq k$ which corresponds the outward-directed transfers. The inward-directed transfers can be determined by applying the reciprocity relations given in

Section 3.

Case 1: $k' < k$, $\Sigma^t_{k'} \neq 0$ and $\Sigma^t_k \neq 0$

This case occurs most frequently in practical problems. The escape probability is composed of the following contributions

$$\begin{aligned} C_{k'k} &= \frac{2}{\Sigma^t_{k'} V_{k'}} \int_0^{r_{k'-1}} dy \left[Ki_3(t^+_{k'-1\,k}) - Ki_3(t^+_{k'\,k}) \right] \\ &+ \frac{2}{\Sigma^t_{k'} V_{k'}} \int_0^{r_{k'-1}} dy \left[Ki_3(t^-_{k'\,k}) - Ki_3(t^-_{k'-1\,k}) \right] \\ &+ \frac{2}{\Sigma^t_{k'} V_{k'}} \int_{r_{k'-1}}^{r_{k'}} dy \left[Ki_3(t^-_{k'\,k}) - Ki_3(t^+_{k'\,k}) \right] . \end{aligned} \tag{61}$$

Because of

$$t^+_{k'-1\,k} = t^-_{k'-1\,k}\,, \text{ if } r_{k'-1} \leq y \leq r_{k'} \tag{62}$$

the three terms in Eq. (61) may be combined to the expression

$$C_{k'k} = \frac{2}{\Sigma^t_{k'} V_{k'}} \int_0^{r_{k'}} dy \left[Ki_3(t^+_{k'-1\,k}) - Ki_3(t^+_{k'k}) + Ki_3(t^-_{k'k}) - Ki_3(t^-_{k'-1\,k}) \right] . \tag{63}$$

The remaining integration in Eq. (63) over the variable y is performed by the use of a Gaussian quadrature. When the escape probabilities have been determined, the collision probabilities $P_{k'k}$ are computed by the use of Eq. (44) and the transport coefficients $T_{k'k}$ subsequently by the use of Eq. (36). The quantities $P_{kk'}$ and $T_{kk'}$ are determined by applying the reciprocity relations given in Eqs.(33) and (35).

Case 2: $k' < k$, $\Sigma^t_{k'} = 0$ and $\Sigma^t_k \neq 0$

The escape probability for this situation can be written as the sum of the following three terms

$$\begin{aligned} C_{k'k} &= \frac{2}{V_{k'}} \int_0^{r_{k'-1}} dy\, x_{k'}(y) Ki_2(t^+_{k'-1\,k}) + \frac{2}{V_{k'}} \int_0^{r_{k'-1}} dy\, x_{k'}(y) Ki_2(t^-_{k'\,k}) \\ &+ 2\,\frac{2}{V_{k'}} \int_{r_{k'-1}}^{r'_k} dy\, x_{k'}(y) Ki_2(t^-_{k'\,k}) \end{aligned} \tag{64}$$

One of the last two integrals can be directly added to the second integral. Because of $\Sigma^t_{k'} = 0$, it furthermore holds

$$t^-_{k'\,k} = t^-_{k'-1\,k} = t^+_{k'-1\,k}\,, \text{ if } r_{k'-1} \leq y \leq r_{k'} \tag{65}$$

such that the other integral can be combined with the first integral. Thus, it can be written

$$C_{k'k} = \frac{2}{V_{k'}} \int_0^{r_{k'}} dy\, x_{k'}(y) \left[Ki_2(t^+_{k'-1\,k}) + Ki_2(t^-_{k'\,k}) \right] . \tag{66}$$

The collision probabilities $P_{k'k}$ and the transport coefficients $T_{k'k}$ as well as the corresponding quantities for the transfers $k \to k'$ are obtained in the same manner as in Case 1.

Case 3: $k' < k$, $\Sigma^t_{k'} \neq 0$ and $\Sigma^t_k = 0$

Since the total cross section in the target interval k is zero, it holds for the escape probability that $C_{k'k} = C_{k'k-1}$. Furthermore, the collision probability for this transfer vanishes, i.e.

$$P_{k'k} = 0\,. \tag{67}$$

For this reason, the transport coefficient $T_{k'k}$ has to be calculated directly in this case. The integral in Eq. (34), which defines the transport coefficients, can be evaluated in the following way

$$\begin{aligned} T_{k'k} &= \frac{1}{4\pi V_k} \int_{V_{k'}} dV' \int_{\mathbf{\Omega}} d\mathbf{\Omega} \int_{s_{k-1}}^{s_k} ds\, e^{-\tau(\mathbf{r}', \mathbf{r}_{k-1})} \exp\left[-\Sigma^t_k (s - s_{k-1}) \right] \\ &= \frac{1}{4\pi V_k} \int_{V_{k'}} dV' \int_{\mathbf{\Omega}} d\mathbf{\Omega}\, e^{-\tau(\mathbf{r}', \mathbf{r}_{k-1})} \, (s_k - s_{k-1}) \\ &= \frac{1}{2\pi V_k} \int_{V_{k'}} dV' \int_0^{2\pi} d\omega Ki_1 \left[t(r', \omega) \right] \, x_k(r', \omega)\,, \end{aligned} \tag{68}$$

where $x_k(r', \omega)$ is the projection of the path $s_k - s_{k-1}$ into the x-y plane. The integrations can be performed in the same way as for the escape probability described above. The result is

$$T_{k'k} = \frac{2}{V_k \Sigma^t_{k'}} \int_0^{r_{k'}} dy \left[Ki_2(t^+_{k'-1\,k-1}) - Ki_2(t^+_{k'k-1}) + Ki_2(t^-_{k'k-1}) - Ki_2(t^-_{k'-1\,k-1}) \right] \, x_k(y)\,, \tag{69}$$

where, because of $\Sigma^t_k = 0$, the index $k-1$ in the arguments of the Ki_2 functions may also be replaced by the index k, which corresponds to the notation used in the TOTMOS code. The collision probability $P_{kk'}$ for the inward-directed transfers can be calculated by the use of the relation

$$P_{kk'} = T_{k'k}\, \Sigma^t_{k'} \tag{70}$$

which is obtained by combining Eqs. (33) and (35). The transport coefficient $T_{kk'}$ is determined as in Case 1.

Case 4: $k' < k$, $\Sigma^t_{k'} = 0$ and $\Sigma^t_k = 0$

The escape probability $C_{k'k}$ is obtained in the same way as in Case 3. Since the collision probability $P_{k'k}$ is zero for the situation considered, the transport coefficient $T_{k'k}$ has to be calculated again directly. This is composed of the following contributions

$$\begin{aligned} T_{k'k} &= \frac{2}{V_k}\int_0^{r_{k'-1}} dy\, x_{k'}(y) Ki_1(t^+_{k'-1\,k-1})\, x_k(y) + \frac{2}{V_k}\int_0^{r_{k'-1}} dy\, x_{k'}(y) Ki_1(t^-_{k'\,k-1})\, x_k(y) \\ &+ 2\,\frac{2}{V_k}\int_{r_{k'-1}}^{r_{k'}} dy\, x_{k'}(y) Ki_1(t^-_{k'\,k-1})\, x_k(y)\,. \end{aligned} \tag{71}$$

Because of

$$t^+_{k'-1\,k-1} = t^-_{k'\,k-1}\,,\ \text{if}\ r_{k'-1} \le y \le r_{k'}\,, \tag{72}$$

Eq. (71) can be brought into the form

$$T_{k'k} = \frac{2}{V_k}\int_0^{r_{k'}} dy\, x_{k'}(y) x_k(y) \left[Ki_1(t^+_{k'-1\,k-1}) + Ki_1(t^-_{k'\,k-1})\right]\,, \tag{73}$$

where the index $k-1$ in the arguments of the Ki_1 function may again be replaced by the index k, which corresponds to the notation in the TOTMOS code. The quantities $P_{kk'}$ and $T_{kk'}$ are obtained as in Case 3.

Case 5: $k = k'$, $\Sigma^t_{k'} \neq 0$

The escape probability $C_{k'k'}$ is determined as in Case 1 by applying Eq. (63) where $t^-_{k'k'} = 0$. The collision probability $P_{k'k'}$ can be calculated from balance considerations. A neutron which emerges in the interval k' either has its next collision in k' or leaves this interval through the boundary $A_{k'}$ or experiences its next collision in one of the inner intervals $j < k'$. Thus, the following equation must hold

$$P_{k'k'} + C_{k'k'} + \left(C^i_{k'\,k'-1} - C^a_{k'\,k'-1}\right) = 1\,, \tag{74}$$

where $C^i_{k'\,k'-1}$ is the probability that a neutron which emerges in interval k' reaches the boundary $A_{k'-1}$ without collision and $C^a_{k'\,k'-1}$ is the probability that a neutron which emerges

in interval k' crosses the boundary $A_{k'-1}$ and reaches the boundary $A_{k'-1}$ again after passing through the inner intervals $j < k'$. The expression in parentheses then gives the probability that a neutron which emerges in interval k' experiences its next collision in one of the inner intervals $j < k'$. Thus

$$P_{k'k'} = 1 - C_{k'k'} - \left(C^i_{k'\,k'-1} - C^a_{k'\,k'-1}\right) . \tag{75}$$

The escape probability $C_{k'k'}$ is given in Eq. (63). The probabilities $C^i_{k'\,k'-1}$ and $C^a_{k'\,k'-1}$ are given by

$$C^i_{k'\,k'-1} = \frac{2}{\Sigma^t_{k'} V_{k'}} \int_0^{r_{k'-1}} dy \left[Ki_3(t^-_{k'\,k'}) - Ki_3(t^-_{k'-1\,k'})\right] \tag{76}$$

and

$$C^a_{k'\,k'-1} = \frac{2}{\Sigma^t_{k'} V_{k'}} \int_0^{r_{k'-1}} dy \left[Ki_3(t^+_{k'-1\,k'-1}) - Ki_3(t^+_{k'\,k'-1})\right] , \tag{77}$$

where $t^-_{k'\,k'} = 0$. If both expressions are inserted into Eq. (75), the upper integral limits can be extended to $r_{k'}$, since, because of

$$t^+_{k'-1\,k'-1} = t^-_{k'\,k'} \quad \text{and} \quad t^+_{k'\,k'-1} = t^-_{k'-1\,k'} \,, \text{ if } r_{k'-1} \le y \le r_{k'} \,, \tag{78}$$

the added terms cancel each other due to the difference in the parenthesis. After some further conversions the following result is obtained

$$P_{k'k'} = 1 - \frac{2}{\Sigma^t_{k'} V_{k'}}$$
$$\times \int_0^{r_{k'}} dy \left\{2Ki_3(t^+_{k'-1\,k'}) + 2\left[Ki_3(t^-_{k'\,k'}) - Ki_3(t^-_{k'-1\,k'})\right] - Ki_3(t^+_{k'\,k'}) - Ki_3(t^+_{k'-1\,k'-1})\right\} . \tag{79}$$

The transport coefficient $T_{k'k'}$ is calculated again using Eq. (36).

Case 6: $k = k'$ and $\Sigma^t_{k'} = 0$

Since the source interval and the target interval coincide and the corresponding total cross section is zero, the collision probability vanishes, i.e.

$$P_{k'k'} = 0 . \tag{80}$$

The escape probability $C_{k'k'}$ can be written, similar to Case 2, as the sum of three terms

$$\begin{aligned} C_{k'k'} &= \frac{2}{V_{k'}} \int_0^{r_{k'-1}} dy\, x_{k'}(y)\, Ki_2(t^+_{k'-1\,k'-1}) + \frac{2}{V_{k'}} \int_0^{r_{k'-1}} dy\, x_{k'}(y)\, Ki_2(t^-_{k'-1\,k'}) \\ &+ 2\,\frac{2}{V_{k'}} \int_{r_{k'-1}}^{r_k} dy\, x_{k'}(y)\, Ki_2(t^+_{k'\,k'}) . \end{aligned} \tag{81}$$

Since $t^-_{k'-1\,k'} = 0$ and because of

$$t^+_{k'-1\,k'-1} = 0 \quad \text{and} \quad t^+_{k'\,k'} = 0\,, \text{ if } r_{k'-1} \le y \le r_{k'}\,, \tag{82}$$

the integrals in Eq. (85) can again be combined. Thus

$$C_{k'k'} = \frac{2}{V_{k'}} \int_0^{r_{k'}} dy\, x_{k'}(y) \left[Ki_2(t^+_{k'-1\,k'-1}) + Ki_2(0) \right]\,, \tag{83}$$

where $Ki_2(0) = 1$.

Since $P_{k'k'}$ is zero, the transport coefficient $T_{k'k'}$ has to be calculated again in this case. Due to the coincidence of the source interval and the target interval, the integrations over these intervals are no longer independent. The occurring integrals are of the form

$$\int_{\tilde{x}_{k'-1}}^{\tilde{x}_{k'}} dx' \int_{x'}^{\tilde{x}_{k'}} dx = \frac{1}{2}(\tilde{x}_{k'} - \tilde{x}_{k'-1})^2 = \frac{1}{2} x^2_{k'}(y) \tag{84}$$

where $\tilde{x}_{k'-1}$ and $\tilde{x}_{k'}$ are the limits of the variable x for the interval k'. The transport coefficient is composed of the following three terms

$$\begin{aligned} T_{k'k'} &= \frac{2}{V_{k'}} \frac{1}{2} \int_0^{r_{k'-1}} dy\, x^2_{k'}(y)\, Ki_1(t^+_{k'-1\,k'-1}) + \frac{2}{V_{k'}} \frac{1}{2} \int_0^{r_{k'-1}} dy\, x^2_{k'}(y)\, Ki_1(0) \\ &+ 2\, \frac{2}{V_{k'}} \frac{1}{2} \int_{r_{k'-1}}^{r_{k'}} dy\, x^2_{k'}(y)\, Ki_1(0)\,, \end{aligned} \tag{85}$$

where $Ki_1(0) = \pi/2$. Because of

$$t^+_{k'-1\,k'-1} = 0\,, \text{ if } r_{k'-1} \le y \le r_{k'} \tag{86}$$

the terms in Eq. (84) can be combined to the following expression

$$T_{k'k'} = \frac{1}{V_{k'}} \int_0^{r_{k'}} dy\, x^2_{k'}(y) \left[Ki_1(t^+_{k'-1\,k'-1}) + Ki_1(0) \right]\,. \tag{87}$$

5.3 Spherical Geometry

The coordinate systems used in spherical geometry are shown in Fig. 6. The spatial coordinates are denoted by r, ϑ, and φ, where r is the distance to the point $\mathbf{r}$, ϑ the polar angle, and φ the azimuthal angle. The $\hat{\mathbf{e}}_r$-axis of the coordinate system for the direction vector $\mathbf{\Omega}$ points in the direction of the spatial vector $\mathbf{r}$. The polar angle θ of $\mathbf{\Omega}$ is counted

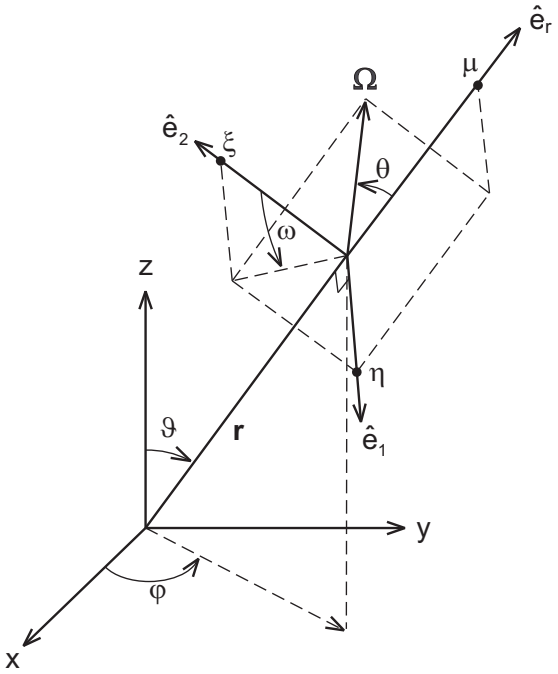

Fig. 6: Coordinates in spherical geometry. (The axis intercepts μ, η, ξ denote the Cartesian coordinates of the direction vector $\mathbf{\Omega}$).

from this axis. Furthermore, the azimuthal angle ω is defined as the angle between the plane formed by the vectors $\hat{\mathbf{z}}$ and $\hat{\mathbf{r}}$ and the plane formed by the vectors $\hat{\mathbf{e}}_r$ and $\mathbf{\Omega}$. The infinitesimal source volume element dV' is given by

$$dV' = r'^2 dr' \sin\vartheta' d\vartheta' d\varphi' \tag{88}$$

and the solid angle element again by

$$d\mathbf{\Omega} = \sin\theta d\theta d\omega \,. \tag{89}$$

The expressions for the volume element and the solid angle element are inserted into Eq. (45). Since the possible flight paths from a source point $\mathbf{r}'$ do not depend on the angle ω, the integration over this variable can be performed. For reasons of symmetry, the problem furthermore does not depend on ϑ' and φ' such that the integrations over these variables can

also be performed. Thus, it may be written

$$\begin{aligned} C_{k'k} &= \frac{1}{2V_{k'}} \int_{V_{k'}} dV' \int_0^{\pi} \sin\theta d\theta \, e^{-\tau} \\ &= \frac{2\pi}{V_{k'}} \int_0^{r_{k'}} r'^2 dr' \int_0^{\pi} \sin\theta d\theta \, e^{-\tau} \,, \end{aligned} \tag{90}$$

where

$$\tau = \tau(r', \theta) = \Sigma_{k'}^t \left[\sqrt{r_{k'}^2 - (r' \sin\theta)^2} - r' \cos\theta \right] + t_{k'k}^* \,. \tag{91}$$

The quantity $t_{k'k}^*$ is again the optical path length from the outer boundary of the interval k' to the outer boundary of the interval k along the direction θ. The symmetry properties of the problem in the case of the spherical geometry have the consequence that the flight paths need only be considered in a plane through the sphere which contains the source point $\mathbf{r}'$ and the center of the sphere. Thus, the flight paths can be treated by the use of the same scheme as in the case of cylindrical geometry with the sole difference that instead of the azimuthal angle ω the polar angle θ is used as the angle variable. Similar to the case of the cylindrical geometry, the variable transformations

$$\begin{aligned} x &= r' \cos\theta' - r_{k'} \cos\theta_{k'} \\ y &= r' \sin\theta' \end{aligned} \tag{92}$$

are made, where $\theta_{k'}$ denotes the polar angle at the position at which the flight path intersects the outer boundary of the interval k'. Furthermore, it follows

$$r'^2 \sin\theta' dr' d\theta' = y dx dy \,. \tag{93}$$

If $a(y)$ again denotes the length of the chord or of a section of the chord which intersects the interval k' at the distance y, the escape probability can be written in the form

$$C_{k'k} = \frac{2\pi}{V_{k'}} \int_0^{r_{k'}} y \, dy \int_0^{a(y)} dx \, \exp - \left\{ \Sigma_{k'}^t \left[a(y) - x \right] + t_{k'k}^* \right\} \,. \tag{94}$$

In order to simplify the integral, the variable transformation $y' = y^2$ with $dy' = 2ydy$ is made. If the quantity y' is subsequently again denoted by y and if the variable x and the section $a(y)$ are again given in mean free paths, the following is obtained

$$C_{k'k} = \frac{\pi}{V_{k'} \Sigma_{k'}^t} \int_0^{r_{k'}^2} dy \int_0^{a(y)} dx \, \exp - \left\{ \left[a(y) - x \right] + t_{k'k}^* \right\} \,. \tag{95}$$

The integration over x gives

$$C_{k'k} = \frac{\pi}{V_{k'}\Sigma^t_{k'}} \int_0^{r^2_{k'}} dy \left\{\exp(-t^*_{k'k}) - \exp - [a(y) + t^*_{k'k}]\right\} . \tag{96}$$

It is seen that the structure of the integral is the same as that in Eq. (58) for the cylindrical geometry except that the integrand contains the exponential function instead of the Bickley function. Thus, the computation of the collision probabilities in spherical geometry can be made by the same procedure as is used in cylindrical geometry.

If, for example, the Case 1 in Section 5.2 with $k' \neq k$ and $\Sigma^t_{k'} \neq 0$ and $\Sigma^t_k \neq 0$ is considered, the following expression is obtained for the escape probability in spherical geometry

$$C_{k'k} = \frac{\pi}{V_{k'}\Sigma^t_{k'}} \int_0^{r^2_{k'}} dy \left(e^{-t^+_{k'-1k}} - e^{-t^+_{k'k}} + e^{-t^-_{k'k}} - e^{-t^-_{k'-1k}}\right) , \tag{97}$$

where the remaining integration over y is again solved numerically by a Gaussian quadrature. The results for the other cases can be taken over analogously.

5.4 Albedo Boundary Condition

The above procedure for calculating the collision probabilities also enables an albedo boundary condition at the outer boundary of the system under consideration to be readily accounted for.[8,9] The albedo concept states that a fraction of the particles which leave the system, re-enter the system through the outer boundary A with an isotropic angular distribution. The escape probability that a particle which emerges in the interval k leaves the system without collision is $C_{k\,K}$, which will be denoted in the following by $C_{k\,A}$. If α is the albedo at the outer boundary, which may be a function of the energy, the fraction $\alpha\, C_{k\,A}$ will re-enter the system.

If the incoming angular flux at the outer boundary A is denoted by $\Phi(\mathbf{r}_A, \mathbf{\Omega})$, the incoming current density is $\mathbf{j}(\mathbf{r}_A, \mathbf{\Omega}) = \mathbf{\Omega}\,\Phi(\mathbf{r}_A, \mathbf{\Omega})$. If, furthermore, $\mathbf{n}_A$ denotes the outward-directed unit vector normal to the surface A and dA an infinitesimal surface element on A, the total number of particles re-entering the system is given by

$$\begin{aligned} \int_A \int_{\mathbf{\Omega}} \mathbf{j}(\mathbf{r}_A, \mathbf{\Omega}) d\mathbf{A} d\mathbf{\Omega} &= \int_A \int_{\mathbf{\Omega}} (\mathbf{n}_A \cdot \mathbf{\Omega}) \Phi(\mathbf{r}_A, \mathbf{\Omega}) dA d\mathbf{\Omega} \\ &= \Phi(\mathbf{r}_A, \mathbf{\Omega})\, \pi A\,, \end{aligned} \tag{98}$$

where the $\mathbf{\Omega}$ integration has been performed over the incoming directions $\mathbf{n}_A \cdot \mathbf{\Omega} < 0$. If the number of particles re-entering the system is unity, the incoming angular flux is given by

$$\Phi(\mathbf{r}_A, \mathbf{\Omega}) = \frac{1}{\pi A} \tag{99}$$

and the incoming current density by

$$\mathbf{j}(\mathbf{r}_A, \mathbf{\Omega}) = \frac{\mathbf{\Omega}}{\pi A}\,. \tag{100}$$

The probability $P_{A\,k}$ that a particle which re-enters the system across the boundary A experiences its next collision in the interval k is thus given by

$$P_{Ak} = \frac{1}{\pi A} \int_A \int_{\mathbf{\Omega}} \int_s (\mathbf{n}_A \cdot \mathbf{\Omega}) e^{-\tau(\mathbf{r}_A, \mathbf{r})}\, \Sigma_t(\mathbf{r})\, dA d\mathbf{\Omega} ds\,, \tag{101}$$

where the integrations over the incoming direction $\mathbf{\Omega}$ and the spatial variable s have to be performed in such a way that all points in the interval k are covered. It is convenient for this reason to again replace the integration over s and $\mathbf{\Omega}$ by a volume integration over the interval k, where

$$dV = |\mathbf{r} - \mathbf{r}_A|^2\, ds d\mathbf{\Omega}\,.$$

In order to perform the integration over the surface A, the origin of the coordinate system is shifted into the target point $\mathbf{r}$. The surface integration is then replaced by an integration over all directions. With

$$d\mathbf{\Omega}_A = \frac{(\mathbf{n}_A \cdot \mathbf{\Omega}) dA}{|\mathbf{r}_A - \mathbf{r}|^2} \tag{102}$$

and

$$\tau(\mathbf{r}_A, \mathbf{r}) = \tau(\mathbf{r}, \mathbf{r}_A) \tag{103}$$

the following result is obtained

$$\begin{aligned} P_{Ak} &= \frac{\Sigma_k^t}{\pi A} \int_{V_k} dV \int_{4\pi} d\mathbf{\Omega}_A\, e^{-\tau(\mathbf{r}, \mathbf{r}_A)} \\ &= \frac{4\Sigma_k^t V_k}{A}\, C_{kA}\,, \end{aligned} \tag{104}$$

where it has again been assumed that the total cross section $\Sigma_t(\mathbf{r})$ is constant in the interval k. By the albedo boundary condition, the collision probability $P_{k'k}$ for the vacuum boundary

condition is increased due to the returning particles. If one re-enter process is regarded for the first instance, the new collision probability $P^*_{k'k}$ is given by

$$P^*_{k'k} = P_{k'k} + \alpha\, C_{k'A}\, P_{Ak}\,. \tag{105}$$

A fraction of the particles which re-enter the system through the outer surface A crosses the system without collision. The probability C_{AA} for this process may be expressed by

$$C_{AA} = 1 - \sum_{k=1}^{K} P_{Ak}\,. \tag{106}$$

The fraction α of these particles re-enters the system again and can experience a collision in the interval k. This process is repeated infinitely. Thus, the collision probability $P^*_{k'k}$ can be written as an infinite sum

$$\begin{aligned} P^*_{k'k} &= P_{k'k} + \alpha\, C_{k'A}\, P_{Ak} + \alpha^2\, C_{k'A}\, C_{AA}\, P_{Ak} + \cdots + \alpha^m\, C_{k'A}\, (C_{AA})^{m-1}\, P_{Ak} + \cdots \\ &= P_{k'k} + \alpha\, C_{k'A} P_{Ak} \left[1 + \alpha\, C_{AA} + \cdots + \alpha^{m-1}\, (C_{AA})^{m-1} + \cdots\right]\,. \end{aligned} \tag{107}$$

If $\alpha\, C_{AA} < 1$, the sum converges and the resulting collision probability may be written as

$$P^*_{k'k} = P_{k'k} + \frac{\alpha\, C_{k'A}\, P_{Ak}}{1 - \alpha\, C_{AA}}\,. \tag{108}$$

If the additional term in Eq. (108) is expressed in terms of escape probabilities only, the following result is obtained

$$P^*_{k'k} = P_{k'k} + \alpha C_{k'A}\, \frac{\gamma_k C_{kA}}{1 - \alpha \left(1 - \sum\limits_{n=1}^{K} \gamma_n C_{nA}\right)}\,, \tag{109}$$

where

$$\gamma_k = \frac{4}{A} \Sigma^t_k V_k\,. \tag{110}$$

5.5 Application of the Reciprocity Relation and Normalization

The collision probabilities $P_{k'k}$ are explicitly calculated for the outgoing directions, i.e. for $k' = 1, 2, \cdots, K$ and $k = k', k'+1, \cdots, K$. These are the terms which appear in the matrix in Table I on the diagonal and below the diagonal. The remaining collision probabilities for $k' = 2, 3, \cdots, K$ and $k = 1, 2, \cdots, k'-1$ above the diagonal are determined by applying the reciprocity relation given in Eq. (33).

Table I

Matrix of the spatial transitions $k' \to k$.

k	$k'=1$	$k'=2$	$k'=3$	$\cdots$	$k'=K$
1	$1 \to 1$	$2 \to 1$	$3 \to 1$	$\cdots$	$K \to 1$
2	$1 \to 2$	$2 \to 2$	$3 \to 2$	$\cdots$	$K \to 2$
3	$1 \to 3$	$2 \to 3$	$3 \to 3$	$\cdots$	$K \to 3$
.	$\cdots$				
K	$1 \to K$	$2 \to K$	$3 \to K$	$\cdots$	$K \to K$.

A particle which emerges in interval k' either experiences a collision in one of the intervals $k = 1, 2, \cdots, K$ or leaves the system without collision. Thus, the condition

$$\sum_{k=1}^{K} P_{k'k} + C_{k'A} = 1 \tag{111}$$

must be satisfied for each source interval k' and its fulfillment represents the degree of accuracy with which escape probabilities and the collision probabilities are calculated. The condition in Eq. (111) represents a particle balance and is therefore of crucial importance for the convergence behavior of the numerical method used for the solution of the collision equations. For this reason, the collision probabilities $P_{k'k}$ and the escape probability $C_{k'A}$ are normalized in order to force Eq. (111) to be satisfied.

The following procedure is used for the normalization process in the TOTMOS code. For $k' = 1$ the collision probabilities P_{1k} are normalized by the reciprocal of Eq. (111). The terms $P_{k'1}$ are then calculated for $k' = 2, 3, \cdots, K$ by applying the reciprocity relation. If Eq. (111) is written in the form

$$\sum_{k=k'}^{K} P_{k'k} + C_{k'A} = 1 - \sum_{k=1}^{k'-1} P_{k'k} \tag{112}$$

and the above procedure is continued successively for the other values of k', the right side of the equation is already normalized and in this sense correct such that the normalization factors

$$f_{k'} = \frac{1 - \sum\limits_{k=1}^{k'-1} P_{k'k}}{\sum\limits_{k=k'}^{K} P_{k'k} + C_{k'A}} \,, \qquad k' = 2, 3, \cdots, K \tag{113}$$

may be used in order to normalize the remaining collision probabilities for the transfers in the diagonal and below the diagonal of the matrix in Table I and the escape probability $C_{k'A}$.

6 ITERATION TECHNIQUES

6.1 Power Iteration Method and Source Iterations

As next step, the collision equations are brought into the multigroup form. The neutron energy range of interest is divided into a finite number, G, of energy intervals or groups, which are separated by the energies E_g, where $g = 1, 2, \cdots, G$. The order of numbering is such that as g increases, the energy decreases, i.e $E_g > E_{g+1}$. The energy-dependent fluxes and cross sections in Eq. (25) are then replaced by the corresponding group-averaged quantities. If the collision probabilities in Eq. (25) are furthermore expressed by the transport coefficients, the following equations are obtained

$$\begin{aligned} \Phi_{k\,g} &= \sum_{k'} T_{k'k\,g}\, Q_{k'g} \\ &= \sum_{k'} T_{k'k\,g}(F_{k'g} + \sum_{g'} \Sigma^s_{k'g'\to g}\Phi_{k'g'}) \\ &= \sum_{k'} T_{k'k\,g}(F_{k'g} + \sum_{g'} P_{k'g'g}\Phi_{k'g'})\,, \end{aligned} \tag{114}$$

where the nomenclature has been changed by replacing $\Sigma^s_{k'\,g'\to g}$ by $P_{k'g'g}$ in order to simplify the notation.[b] The summation index k' in Eq. (114) runs from 1 to K and the index g' over all groups from 1 to G. The summation indices are not explicitly given in Eq. (114) and the following equations for the sake of simplicity. In order to discuss the iteration techniques used to solve the integral transport equation, it is convenient to write Eq. (111) in a symbolic notation, i.e.

$$\mathbf{\Phi} = \mathbf{T}(\mathbf{F} + \mathbf{P}\mathbf{\Phi})\,. \tag{115}$$

where the array $\mathbf{\Phi}$ is defined by

$$\mathbf{\Phi} = \begin{pmatrix} \mathbf{\Phi}_1 \\ \mathbf{\Phi}_2 \\ \vdots \\ \mathbf{\Phi}_G \end{pmatrix} \quad \text{with} \quad \mathbf{\Phi}_g = \begin{pmatrix} \Phi_{1g} \\ \Phi_{2g} \\ \vdots \\ \Phi_{Kg} \end{pmatrix}\,. \tag{116}$$

[b] The simultaneous use of the capital letter P for the collision probability in the previous sections should not lead to confusion, since the latter is not dealt with in this section.

The matrices $\mathbf{T}$, $\mathbf{F}$, and $\mathbf{P}$ can be defined in a similar way.

The total fission source is normalized to unity. If $\mathbf{A}$ denotes the absorption operator (or absorption plus leakage operator, if the vacuum or the albedo boundary condition is used) the normalization condition for the fluxes is

$$\mathbf{A}\mathbf{\Phi} = 1\,. \tag{117}$$

If a conserving boundary condition is used at the outer boundary of the system, the absorption operator is defined by

$$\mathbf{A}\mathbf{\Phi} = \sum_{k,\,g} V_k \Sigma^a_{k\,g} \Phi_{k\,g}\,, \tag{118}$$

where $\Sigma^a_{k\,g}$ is the absorption cross section in the interval k and the energy group g. If a vacuum or an albedo boundary condition is used, it must hold that

$$\mathbf{A}\mathbf{\Phi} = \sum_{k,\,g'} V_k \Phi_{k\,g'} \left(\Sigma^t_{k\,g'} - \sum_g q_{kg} P_{kg'g} \right)\,. \tag{119}$$

Eq. (115) is solved by flux and source iterations. During the flux iterations the fission source is kept constant. The flux is calculated by the use of the power iteration method. This method is characterized by a trial solution $\mathbf{\Phi}^n$ being inserted into the right side of Eq. (115), which gives a new improved solution $\mathbf{\Phi}^{n+1}$, i.e.

$$\mathbf{\Phi}^{n+1} = \mathbf{T}(\mathbf{F} + \mathbf{P}\mathbf{\Phi}^n)\,. \tag{120}$$

At the beginning of the iterations a flux estimate and an estimate of the initial eigenvalue is made, with which the initial neutron source in the system under consideration is calculated.

The flux iterations start with the first energy group and the fluxes $\mathbf{\Phi}_1$ are determind by the use of Eq. (120) on the assumption that the fission source is known and constant. The procedure is continued gradually for all further groups $g = 2, 3, \cdots, G$. Subsequently, the scattering source $\mathbf{P}\Phi$ is recalculated and the power iterations are started again. If the relative difference of all fluxes $\mathbf{\Phi}$ in two subsequent iterations is smaller than a given value (normally 10^{-4}) the flux iterations are assumed to have converged. A complete run through all groups is called a source (or outer) iteration.

With each outer iteration the fission source is recalculated and a new eigenvalue

$$k_{eff} = \frac{\text{productions}}{\text{absorptions} + \text{leakage}} = \frac{< \nu\Sigma_f\Phi >}{< \Sigma_a\Phi > + L} \tag{121}$$

is determined, where the symbol <> stands for the spatial integration over the whole system considered and the integration over all energies. This corresponds in the TOTMOS code to a volume weighted summation over all spatial intervals and a summation over all energy groups. The quantity L is the leakage out of the system. The k-eigenvalue is used to correct the fission source in order to keep the total number of neutrons in the system nearly constant. If the relative difference of the fission source in two subsequent iterations is smaller than a given value (normally 10^{-5}) the outer iterations are assumed to have converged and the iteration procedure is terminated.

If $\mathbf{\Phi}^{\infty}$ is the exact solution to the problem, the difference $\boldsymbol{\epsilon}^n = \mathbf{\Phi}^n - \mathbf{\Phi}^{\infty}$ is the error in the flux calculation after the nth iteration. In order to study the convergence behavior of the power iteration method, it is convenient to expand the fluxes in terms of the eigenfunctions of the operator $\mathbf{TP}$, which are defined by

$$\mathbf{TP}\mathbf{\Psi} = \lambda\mathbf{\Psi}\,. \tag{122}$$

The eigenvalues of Eq. (122) are denoted in the following by λ_i and the eigenfunctions by $\mathbf{\Psi}_i$. For the following considerations, the eigenvalues are ordered such that $\lambda_1 > \lambda_2 > \lambda_3 > \cdots$. The largest eigenvalue λ_1 is called the spectral radius of the operator $\mathbf{TP}$. The error $\boldsymbol{\epsilon}^n$, the term $\mathbf{TF}$, and the solution $\mathbf{\Phi}^{\infty}$ are now represented by the following series expansions

$$\boldsymbol{\epsilon}^n = \sum_{i=1}^{\infty} a_i^n \mathbf{\Psi}_i \tag{123}$$

$$\mathbf{TF} = \sum_{i=1}^{\infty} b_i \mathbf{\Psi}_i \tag{124}$$

and

$$\mathbf{\Phi}^{\infty} = \sum_{i=1}^{\infty} c_i \mathbf{\Psi}_i\,. \tag{125}$$

The iteration with $\mathbf{\Phi}^{\infty}$ should reproduce itself, such that the equation

$$\mathbf{\Phi}^{\infty} = \mathbf{T}(\mathbf{F} + \mathbf{P}\mathbf{\Phi}^{\infty}) \tag{126}$$

should be fulfilled. If the series expansions in Eqs.(124) and (125) are inserted into Eq. (126), the solution $\mathbf{\Phi}^{\infty}$ can be expressed by

$$\mathbf{\Phi}^{\infty} = \sum_{i=1}^{\infty} \frac{b_i}{1-\lambda_i} \mathbf{\Psi}_i\,. \tag{127}$$

Because of

$$\boldsymbol{\epsilon}^{n+1} = \mathbf{TP}\boldsymbol{\epsilon}^{n}\,, \tag{128}$$

the error after the nth iteration may be written as

$$\begin{aligned} \boldsymbol{\epsilon}^{n} &= (\mathbf{TP})^{n}\boldsymbol{\epsilon}^{0} \\ &= (\mathbf{TP})^{n}\sum_{i=1}^{\infty} a_i^0 \boldsymbol{\Psi}_i \\ &= \sum_{i=1}^{\infty} a_i^0 (\lambda_i)^n \boldsymbol{\Psi}_i\,. \end{aligned} \tag{129}$$

The error goes to zero, if it holds for all eigenvalues that $\lambda_i < 1$. Since λ_1 is the largest eigenvalue, the contribution of the higher modes to the error will be small compared to the first mode after a sufficiently large number of iterations. Thus, for large n the error will approximately decay as

$$\boldsymbol{\epsilon}^{n} \approx a_1^0 (\lambda_1)^n \boldsymbol{\Psi}_1 = a_1^0 e^{n \ln \lambda_1} \boldsymbol{\Psi}_1\,. \tag{130}$$

The term $e^{ln\,\lambda_1}$ is the decay factor for the error and

$$v = -\ln \lambda_1\,. \tag{131}$$

is denoted as the decay rate of the iteration. The quantity a_1^0 is the difference between the amount of the first mode in the initial vector $\boldsymbol{\Phi}^0$ and the exact solution vector $\boldsymbol{\Phi}^\infty$.

If the Eq. (122) for the eigenvalue λ_1 is multiplied by the total cross section and integrated over the cell volume and the whole energy range, it is seen that λ_1 can be interpreted as the ratio of the number of collisions in the first mode due to neutrons emerged in scattering processes to the total number of collisions in the first mode. Thus, the value of the first eigenvalue depends on whether the neutrons which make a collision originate directly from the fission source or whether they have undergone one or more scattering processes. This system property may be described by the quantity Σ_s/Σ_t, which is therefore also denoted as dominance ratio in the context of the convergence behavior of the power iteration method. For weakly absorbing systems, as for example graphite-moderated systems, the value of Σ_s/Σ_t is close to unity such that the error decays only slowly in this case.

In order to accelerate the convergence of the power iteration method, the TOTMOS code applies the same techniques as those used in the THERMOS code. These techniques

are renormalization (or scaling),[19] over-relaxation,[20] and extrapolation,[21], which will be described in the following.

6.2 Renormalization

The first technique applied in the TOTMOS code for accelerating the convergence is renormalization. The basis for this technique is the experience that the convergence rate can be improved if the particle balance in the system is fulfilled during the iteration steps. If the iterated flux $\mathbf{\Phi}^n$ is normalized in the sense that $\mathbf{A}\mathbf{\Phi}^n = 1$, the new flux $\mathbf{\Phi}^{n+1}$ will not in general be normalized. For this reason, the iteration equation is changed in order to force the particle balance to be correct on the average, i.e.

$$\mathbf{\Phi}^{n+1} = \frac{\mathbf{T}(\mathbf{F} + \mathbf{P}\mathbf{\Phi}^n)}{\mathbf{A}\mathbf{T}(\mathbf{F} + \mathbf{P}\mathbf{\Phi}^n)} \,. \tag{132}$$

The convergence behavior of the modified iteration equation can be analyzed again by using the eigenfunction expansion of the error $\boldsymbol{\epsilon}^n$. With

$$\mathbf{\Phi}^n = \mathbf{\Phi}^\infty + \boldsymbol{\epsilon}^n \tag{133}$$

Eq. (132) can be written in the form

$$\mathbf{\Phi}^\infty + \sum_{i=1}^{\infty} a_i^{n+1} \mathbf{\Psi}_i = \frac{\mathbf{\Phi}^\infty + \sum_i a_i^n \lambda_i \mathbf{\Psi}_i}{1 + \sum_j a_j^n \lambda_j \mathbf{A}\mathbf{\Psi}_j} \,. \tag{134}$$

If the errors are small after a sufficiently large number of iterations and the renormalization is near unity, the denominator of Eq. (134) can be expanded. If the terms in the expansion which are quadratic and of a higher order in the error are neglected a comparison of the coefficents on both sides of Eq. (134) yields

$$a_i^{n+1} = a_i^n \lambda_i (1 - \alpha_i) \,, \tag{135}$$

where

$$\alpha_i = b_n \frac{\mathbf{A}\mathbf{\Psi}_i}{1 - \lambda_i} \,. \tag{136}$$

The α_i give the fraction of the neutrons absorbed in the ith mode, since

$$\mathbf{A}\mathbf{\Phi}^\infty = \sum_{i=1}^{\infty} \alpha_i \,. \tag{137}$$

It is reasonable to expect that the lowest eigenfunction $\mathbf{\Psi}_1$ is positive everywhere and that $\mathbf{\Psi}_2$ and the other eigenfunctions have one or more zeros and change sign. Most of the absorptions would then occur in the first mode such that $\alpha_1 \approx 1$ and the other α_i are small. In weakly absorbing systems with $\lambda_1 \approx 1$ this is particularly true. If the source is everywhere positive, α_1 is positve and the convergence is accelerated. It is observed in actual calculations that after many iterations the errors resemble the expected behavior of $\mathbf{\Psi}_2$ so that

$$\lambda_1(1-\alpha_1) < \lambda_2(1-\alpha_2) > \lambda_i(1-\alpha_i),\ i = 3,\, 4, \cdots \tag{138}$$

with the result that the errors decay like $\lambda_2^n(1-\alpha_2)^n$. Thus, the effect of the renormalization is to eliminate the $\mathbf{\Psi}_1$ component of the error. The decay of the error then occurs with $\lambda_2(1-\alpha_2)$ instead of with λ_1.

6.3 Over-Relaxation

The flux vector changes in one iteration by the amount

$$\mathbf{R}^n = \mathbf{\Phi}^{n+1} - \mathbf{\Phi}^n\,. \tag{139}$$

The quantity $\mathbf{R}^n$ is called the residual vector. For the purpose of speeding up the convergence of the iteration the solution is overcorrected (or perhaps undercorrected) by an amount ω. The iteration equation might then be written in the form

$$\begin{aligned} \mathbf{\Phi}^{n+1} &= \mathbf{\Phi}^n + \omega\mathbf{R}^n \\ &= (1-\omega) + \omega\mathbf{T}(\mathbf{F} + \mathbf{P}\mathbf{\Phi}^n)\,, \end{aligned} \tag{140}$$

where ω is a real number. The iteration procedure is called over-relaxation for $\omega > 1$ and under-relaxation for $\omega < 1$. In order to find a value for ω by which the convergence rate is improved it is convenient to express the error of the iteration procedure in terms of the eigenfunctions of the operator $(1-\omega)\mathbf{I} + \omega\mathbf{TP}$, which are defined by

$$\left[(1-\omega)\mathbf{I} + \omega\mathbf{TP}\right]\mathbf{\Psi} = \mu\mathbf{\Psi}\,, \tag{141}$$

where $\mathbf{I}$ is the unit matrix. By rearranging, Eq. (141) can be brought into the form

$$\mathbf{TP}\mathbf{\Psi} = \frac{\mu+\omega-1}{\omega}\mathbf{\Psi}\,. \tag{142}$$

The eigenfunctions of the Eq. (142) are thus again the functions $\mathbf{\Psi}_i$. The eigenvalues μ_i are given by

$$\mu_i = \omega\lambda_i - \omega + 1\,. \tag{143}$$

The error may then be written as

$$\boldsymbol{\epsilon}^n = \sum_{i=1}^{\infty} a_i^0(\omega\lambda_i - \omega + 1)^n \mathbf{\Psi}_i\,. \tag{144}$$

Assuming that the spectral radius is $\mu_1 = \omega\lambda_1 - \omega + 1$, the error approximately decays for large values of n as

$$\boldsymbol{\epsilon}^n \approx a_1^0(\omega\lambda_1 - \omega + 1)^n \mathbf{\Psi}_1\,. \tag{145}$$

The value of ω which eliminates this component of the error is $\omega = 1/(1-\lambda_1)$. The iteration procedure which uses this value of ω is called an extrapolation. It has been observed that by the use of a straightforward power iteration the shape of the residuals $\mathbf{R}^n$ remains the same but that they are reduced after many iterations by the factor μ_1 for each iteration, i.e.

$$\begin{aligned}
\mathbf{\Phi}^{n+1} &= \mathbf{\Phi}^n + \mathbf{R}^n \\
\mathbf{\Phi}^{n+2} &= \mathbf{\Phi}^{n+1} + \mathbf{R}^n \\
&= \mathbf{\Phi}^n + \mathbf{R}^n(1+\mu_1) \\
\mathbf{\Phi}^{n+3} &= \mathbf{\Phi}^n + \mathbf{R}^n(1+\mu_1+\mu_1^2) \\
\vdots &= \qquad\qquad \vdots \\
\mathbf{\Phi}^{\infty} &= \mathbf{\Phi}^n + \mathbf{R}^n/(1-\mu_1)\,.
\end{aligned} \tag{146}$$

Thus, one can extrapolate to an infinite number of iterations if the shape of the residuals and the rate at which their level is changed are known. If the observed behavior of the residuals concerning their shape and decay were exact and if there were no contamination from higher modes the extrapolation procedure would lead to the exact solution. However, even if the initial error vector were orthogonal to the eigenfunction, say $\mathbf{\Psi}_j$, belonging to the eigenvalue μ_j, round-offs in computations would introduce components along $\mathbf{\Psi}_j$ and influence the convergence rate. This means that a value for ω must be found which refines the solution by also eliminating the contamination by all higher modes.

After extrapolating the solution an appropriate value for ω thus has to be sought for in order to refine the solution. If large values of the index i are considered, then μ_i approaches $1-\omega$, since $\lambda_i \to 0$ for large values of i. Thus, $|\mu_i|$ may be greater than unity and the higher modes will grow. As the best value of ω that value ω_b is chosen for which $|\mu_1| = |\mu_i|$, when $i \to \infty$, i.e.

$$\omega_b \lambda_1 - \omega_b + 1 = \omega_b - 1 \tag{147}$$

or

$$\omega_b = \frac{2}{2 - \lambda_1} \,. \tag{148}$$

It is seen from Eq. (148) that the permissible range of ω_b is $1 \leq \omega_b < 2$. The best decay rate that can be obtained is then

$$\mu_b = \omega_b - 1 = \frac{\lambda_1}{2 - \lambda_1} \,. \tag{149}$$

When the renormalization and the over-relaxation techniques are combined, the following iteration equation is obtained

$$\mathbf{\Phi}^{n+1} = \mathbf{\Phi}^n + \omega \left[\frac{\mathbf{T}(\mathbf{F} + \mathbf{P}\mathbf{\Phi}^n)}{\mathbf{A}\mathbf{T}(\mathbf{F} + \mathbf{P}\mathbf{\Phi}^n)} - \mathbf{\Phi}^n \right] . \tag{150}$$

The error after the nth iteration is

$$\boldsymbol{\epsilon}^n = \sum_{i=1}^{\infty} a_i^0 (\mu_i)^n \mathbf{\Psi}_i \,, \tag{151}$$

where the eigenvalues μ_i are given by

$$\mu_i = 1 - \omega + \omega \lambda_i (1 - \alpha_i) \,. \tag{152}$$

The spectral radius is given again by the largest eigenvalue, i.e. by

$$\mu_k = \max(|\mu_1|, |\mu_2|, \cdots, |\mu_i|, \cdots) \,, \tag{153}$$

such that the error decays for large n approximately as

$$\boldsymbol{\epsilon}^n \approx a_k^0 (\mu_k)^n \mathbf{\Psi}_k \,. \tag{154}$$

In practice, the final solution is not known and hence nor is the error at the current iteration. However, the residuals are calculable at any stage of the iteration. The residual vector represents the error vector in a transformed space and the convergence criteria for the residuals

are the same as those for the errors. Furthermore, the asymptotic behavior is the same. Thus

$$\mathbf{R}^{n+1} = \frac{1}{\omega}(\mathbf{\Phi}^{n+1} - \mathbf{\Phi}^n) = \frac{1}{\omega}(\boldsymbol{\epsilon}^{n+1} - \boldsymbol{\epsilon}^n) \tag{155}$$

and

$$\mathbf{R}^{n+1} \to \frac{1}{\omega}(\mu_k - 1)(\mu_k)^n \mathbf{\Psi}_k \,, \tag{156}$$

The approximate behavior of $\mathbf{R}^{n+1}$ can be used as a basis for determining the spectral radius μ_k. It is found in practice that a reliable estimate of μ_k can be obtained by using an averaged value of the residuals, i.e. by using the approximate behavior

$$\left\langle \mathbf{R}^{n+1} \right\rangle / \left\langle \mathbf{R}^n \right\rangle \to \mu_k \,, \tag{157}$$

where

$$\left\langle \mathbf{R}^n \right\rangle = \left[\sum_{k,g} (A_{k\,g} R^n_{k\,g})^2 / \sum_{k,g} (A_{k\,g})^2 \right]^{1/2} . \tag{158}$$

Here, the $A_{k\,g}$ are the elements of the matrix $\mathbf{A}$ defined by Eqs.(118) or (119). Since the fluxes are normalized at any iteration step, it holds

$$\mathbf{A}\mathbf{R}^n = \sum_{k,g} A_{k\,g} R^n_{k\,g} = 0 \,. \tag{159}$$

The complete iteration process is then performed by the use of the following scheme. Eq. (150) is iterated with an initial value ω_0 and the quantity

$$\omega_e = \frac{1}{1 - \mu_k} \tag{160}$$

is computed at each iteration. If the relative deviations of the ω_e from ℓ_e subsequent iterations agree within a given range ϵ_e, the iteration with the current ω value is stopped and an extrapolation is made using the most recent value of ω_e. The value $\lambda^*_k = \lambda_k(1 - \alpha_k)$ is determined from

$$\lambda^*_k = \frac{\mu_k - 1 + \omega_0}{\omega_0} \tag{161}$$

and a new ω is computed by the use of $\omega_1 = 2/(2 - \lambda^*_k)$. If $\omega_1 < 2$, the iteration is continued with the new value, otherwise the iteration is carried on with the previous ω value until the condition is fulfilled. The process is repeated until the residuals $R^{n+1}_{k\,g}$ are less than $\epsilon_r \Phi^n_{k\,g}$ for all values of k and g, where ϵ_r is the convergence criterion for the flux.

For the iteration parameters ω_0, ℓ_e, ϵ_e, and ϵ_r default values are given in the TOTMOS code which may be replaced by other values in the input. Testing for a possible extrapolation is not made during the first ℓ_b iterations nor during the ℓ_d iterations after an extrapolation. For the quantities ℓ_b and ℓ_d default values also exist, which may be changed in the input.

7 CROSS SECTION DATA

7.1 General Considerations

The TOTMOS code has been designed to process three different types of cross section data. The standard procedure is to use complete sets of tabulated multigroup cross sections, which are given in the format of the library used in the MUPO code. These data are computed by separate programs, transformed into the MUPO library format and stored for later use in the TOTMOS code.

For those nuclides for which no chemical binding effects have to be taken into acccount, the free-gas kernel model can be applied in order to calculate the one-dimensional thermal scattering cross sections and the thermal transfer cross sections. Since the free-gas model is frequently used and easy to compute, it has been incorporated into the TOTMOS code. Here, the free-gas scattering model is employed in the Brown and St. John form, which is described in Section 7.3. The Brown and St. John free-gas scattering kernels are calculated for neutron energies up to 2 eV. These data are averaged by an appropriate weighting function in order to determine the group-to-group transfer cross sections for the free-gas model. The weighting function used is based on the Westcott formalism, which is described in Section 7.4.

The fission products generated in nuclear fission normally have no effect on the scattering properties of the nuclear systems considered. Thus, it is not necessary to calculate the complete group-to-group transfer cross sections for these nuclei. Rather, it is sufficient in this case to give the absorption cross sections and to restrict the transfer cross sections to the self-scatter term, which is set equal to the total scattering cross section. This procedure has been incorporated into the TOTMOS code in order to save computer memory while simultaneously guaranteeing that the particle balance is fulfilled.

7.2 MUPO Cross Section Library

The tabulated cross section data used by the TOTMOS code have to be given on an external device in the format of the MUPO library. The MUPO library uses a 43 group

structure, which consists of 18 groups in the fast and epithermal energy range and 25 groups in the thermal energy range. The energy range considered extends from 0.0025 eV to 10 MeV. The thermal energy limit is at 3.059 eV.

The moderator materials on the MUPO library for which the effects of chemical binding on the cross sections are considered are beryllium oxide, graphite, light water, and heavy water. The scattering matrices for these moderators are given at different temperatures. The TOTMOS code has been programmed so that the scattering matrices can be determined at a specific temperature of interest. For this purpose, the temperatures in the zones of the reactor cell, which contain a moderator material, can be defined in the TOTMOS input. These are then used in order to calculate a volume-averaged moderator temperature. The thermal scattering matrices at this temperature are then determined by interpolation of the temperature-dependent data, which are given on the MUPO library.

Furthermore, the library contains the cross sections for the most important fissionable nuclides. The remaining data given on the MUPO library concern the light materials, structural materials, fission products and non-fissile heavy metals.

The nuclides thorium-232, uranium-238, plutonium-240, and plutonium-242 are treated as explicit resonance nuclides, for which temperature-dependent self-shielded resonance cross sections may be calculated. The procedure for determining the resonance cross sections has been taken from the MUPO code and uses the equivalence principle in order to calculate the resonance cross sections in heterogeneous systems. This means that the same procedures can be used for both homogeneous and heterogeneous systems in order to calculate the shielded flux under the resonance and to determine the corresponding self-shielded resonance cross section.

If the narrow resonance approximation is used, the shielded resonance cross section in group g with the group boundaries E_{g+1} and E_g is given by[1]

$$\sigma^r_{a,g} = \frac{\Sigma_p}{\ln\frac{E_g}{E_{g+1}}} \int_{E_{g+1}}^{E_g} \frac{\sigma^r_a(E)}{\Sigma_T(E)} \frac{dE}{E} \,, \tag{162}$$

where $\Sigma_T(E)$ is the total macroscopic cross section of the system considered. This is given by

$$\Sigma_T(E) = N_a \left[\sigma^r_a(E) + \sigma^r_{n,res}(E) + \sigma^r_{n,int}(E) + \sigma_p\right] \,, \tag{163}$$

where N_a is the atom number density of the absorber, $\sigma_a^r(E)$ the capture cross section of the resonance absorber, $\sigma_{n,res}^r(E)$ the elastic resonance cross section, $\sigma_{n,int}^r(E)$ the interference cross section, and σ_p the total potential scattering cross section of the system per absorber atom. It is additionally assumed in Eq. (162) that the influence of the resonance on the total flux in the group g is negligible. For the two resonance nuclides, tables of resonance cross sections are given on the MUPO library, which depend on the temperature and the potential scattering cross section

$$\sigma_p = \sigma_{pa} + \kappa \frac{N_m}{N_a} \sigma_{pm} \,, \tag{164}$$

where σ_{pa} is the potential scattering cross section of the resonance absorber, σ_{pm} the potential scattering cross section of all admixed moderators, and N_m the atom number density of all admixed moderators. The parameter κ is used in order to describe the heterogeneity property of the system considered. The resonance tables are given at present for five temperatures and for 20 potential scattering cross sections. In principle, a different partition may be chosen. The only limitation is that the total number of temperatures and cross section parameters must be equal to 25. The resonance cross section for a specific temperature and a specific potential cross section is determined by interpolation. A quadratic interpolation is used concerning the temperature and a linear interpolation concerning σ_p. The cross sections of the remaining resonance nuclides on the MUPO library are given in infinite dilution.

The MUPO library, which is available at present for TOTMOS calculations,[22] is based on ENDF/B-VII data[23] and was generated by the use of the cross section processing code NJOY,[24] where the NJOY version 99.269 was employed. The shielded resonance absorption cross sections of Th-232 and U-238 were determined by the ZUT-DGL code.[25] This is an extension of the ZUT code [26] in which escape probabilities for double-heterogeneous configurations in spherical and cylindrical geometries can be calculated. The shielded resonance absorption cross sections of Pu-240 and Pu-242 were calculated for a typical pebble bed configuration as a function of the temperature and the parameter κ by the use of the MCNP4C code.[27]

7.3 Free-Gas Scattering Kernels

The simplest scattering model in the thermal energy range is the free-gas model, in which the thermal motion of the atomic nuclei in a material is described by a monatomic gas at a temperature equal to the material temperature. The scattering cross sections, which are based on the free-gas model, are characterized by the fact that they are frequently used in applications and easy to compute. For this reason, the computation of the free-gas scattering kernel has been incorporated into the TOTMOS code, where the formulation of the free-gas model by Brown and St. John is used.

The free-gas scattering cross section in the Brown and St. John form is represented by the series expansion

$$\sigma_s(v_r) = \sum_{n=1}^{N} \sigma_n \exp(-\kappa_n v_r^2)\,, \tag{165}$$

where v_r is the relative speed between the neutron and the atomic nucleus, and Σ_n and κ_n are parameters chosen such that $\sigma_s(v_r)$ fits the measured scattering cross section. In many practical cases, it is sufficient to use only one term in the series expansion in Eq. (165). In this case, the parameter κ_1 is set equal to zero and σ_1 equal to the scattering cross section at 2 eV.

The scattering kernel in the Brown and St. John form is given by

$$\begin{aligned}\sigma_s(E' \to E) = \sum_{n=1}^{N} \frac{\sigma_n \Theta_n^2 A}{2E'} \frac{\tau_n \beta^2}{\beta^2 + \kappa_n(A+1)} \\ \times \left\{ \exp\left(-\kappa_n \tau_n^2 \frac{E'}{E_0}\right) E1 + \exp -\frac{\beta^2}{A} \left[\frac{E'}{E_0} - \frac{\beta^2 + \kappa_n(A+1)}{\beta^2 + \kappa_n} \frac{E}{E_0}\right] E2 \right\}\end{aligned} \tag{166}$$

where

$$E1 = \operatorname{erf}(\beta\xi_n\sqrt{E'} + \beta\Theta_n\sqrt{E}) \mp \operatorname{erf}(\beta\Theta_n\sqrt{E} - \beta\xi_n\sqrt{E'}) \tag{167}$$

$$E2 = \operatorname{erf}(\beta\Theta_n\sqrt{E'} - \beta\xi_n\sqrt{E}) \pm \operatorname{erf}(\beta\Theta_n\sqrt{E'} + \beta\xi_n\sqrt{E})\,. \tag{168}$$

The remaining parameters are defined by

$$\beta^2 = \frac{A}{kT} E_0 \tag{169}$$

$$\tau_n^2 = \frac{\beta^2}{\beta^2 + \kappa_n} \tag{170}$$

$$\Theta_n = \frac{A+1}{2A}\tau_n^2 \tag{171}$$

$$\xi_n = \tau_n - \Theta_n \,, \tag{172}$$

where $E_0 = kT_0$ and $T_0 = 293.15$ K. Furthermore, $\mathrm{erf}(x)$ is the Gaussian error function

$$\mathrm{erf}(x) = \frac{2}{\sqrt{\pi}} \int_x^\infty e^{-t^2} dt = -\mathrm{erf}(-x) \,. \tag{173}$$

The upper signs in Eqs.(167) and (168) are to be used if $E' < E$ and the lower signs if $E' > E$. If there is no absorption, a thermal equilibrium is established between the up-scattering and the down-scattering processes. The resulting thermal neutron flux is then a Maxwellian distribution at a temperature which is equal to the temperature of the atomic nuclei. In this case, the transfer cross section in Eq. (166) fulfils the condition of the detailed balance, which states that the number of collisions leading from energy E' to energy E, is equal to the number of collisions leading from E to E', i.e.

$$E'\, e^{-E'/kT} \Sigma_s(E' \to E) = E\, e^{-E/kT}\, \Sigma_s(E \to E') \tag{174}$$

The above formula for the free-gas scattering kernel is used in order to calculate the group-to-group transfer cross sections

$$\sigma^s_{g' \to g} = \frac{\int_{g'} \int_g \sigma_s(E' \to E) \Phi(E') dE' dE}{\Phi_{g'}} \tag{175}$$

for the free-gas model, where

$$\Phi_{g'} = \int_{E_{g'+1}}^{Eg'} \Phi(E') dE' \,. \tag{176}$$

As weighting function $\Phi(E)$ the Westcott flux defined in Section 7.4 is used. The group-averaged values are computed in the TOTMOS code by replacing the integrals in Eq. (175) and Eq. (176) by sums. For this purpose, each energy group is subdivided into M subgroups of equal width. The value of M may be defined in the TOTMOS input. The possible values are restricted to the interval $2 \leq M \leq 5$. The cross sections and the fluxes for each subgroup are approximated by their values at the energy midpoints of the subgroups. The within-group cross sections of the scattering matrix are calculated by

$$\sigma^s_{g' \to g'} = \sigma^s_{g'} - \sum_{g \neq g'} \sigma^s_{g' \to g} \,, \tag{177}$$

where $\sigma^s_{g'}$ is the group-averaged scattering cross section for the group g'.

If the free-gas model is used for a nuclide in the thermal energy range, the group-to-group transfer cross sections in the energy range from 2 eV up to 10 MeV are calculated in the TOTMOS code on the assumption that the atomic nuclei by which the neutrons are scattered are at rest and that the scattering is isotropic in the center-of-mass system.

7.4 The Westcott Formalism

There are two situations in which the TOTMOS code requires an estimate of the energy-dependent flux in the reactor cell under consideration. The first is the calculation of the group-to-group transfer cross sections in the TOTMOS code on the basis of the free-gas model, where a weighting function is needed to average the free-gas scattering kernels. The other situation arises at the beginning of the iteration process for solving the transport equation. In this case, a starting flux is required, with which the initial fission source in the reactor cell to be analyzed is calculated.

A quite good flux estimation up to an energy of 2 eV is given by the Westcott formalism. The energy-dependent flux is thus defined by

$$\Phi(E) = \text{const}\left[1 - \frac{2}{\sqrt{\pi}} r \sqrt{\frac{T}{T_0}} \sqrt{E_0} \int_0^\infty \frac{\Delta(E)}{\sqrt{E^3}} dE\right] \frac{\frac{E}{E_0} e^{-\frac{E/E_0}{T/T_0}}}{\sqrt{\frac{T}{T_0}}} + r\Delta(E) \frac{\sqrt{\frac{T}{T_0}}}{\frac{E}{E_0}}\,, \tag{178}$$

where

$$r = \frac{\sqrt{\pi}\bar{\Sigma}_a}{2\xi\bar{\Sigma}_s\sqrt{T/T_0} + 4\sqrt{\mu}\,\bar{\Sigma}_a} \quad \text{with} \quad \mu = 5 \tag{179}$$

and

$$\Delta(E) = \frac{1}{1 - \frac{0.26}{1+(2.131E)^3}} \frac{1}{1 + (\frac{4.95kT}{E})^7}\,. \tag{180}$$

The quantities $\bar{\Sigma}_a$ and $\bar{\Sigma}_s$ are the total absorption cross section and the total scattering cross section of the reactor cell considered. Furthermore, ξ is the mean logarithmic energy loss of a neutron in the cell. The parameter T is the volume-averaged temperature of the system and T_0 is 293.15 K.

The constants required to calculate the Westcott flux are determined in the subroutine WEST. The Westcott flux is used in the subroutines FREEGAS and FLUX.

8 THE MUPO LIBRARY FORMAT

This section describes the structure of the MUPO library. One characteristic of the library in its original form is that an unformatted cross section representation is used. This form of data storage is often chosen when a large amount of data is to be read since it is, compared to the card-image format,[c] a more efficient method which permits faster access to the data and requires less space for storage. In order to enable the exchange of the cross section data betweeen different computer installations, an auxiliary program was written which converts the unformatted library into the card-image format. The cross sections are stored on the MUPO library for increasing energies. The TOTMOS code needs the data starting with the highest energy. The sequence in storing the cross sections is changed in a TOTMOS run during the reading of the MUPO library. The following records are used in order to read the data of the MUPO library.

Record 1 (general information)

The record with the general information is the first record and has the structure

(TXT(I), I=1, 9), NI, NJ, NK, ID

where

TXT - Text describing the library

NI - Number of nuclides for which group-averaged cross sections are given

NJ - Number of resonance nuclides on the library

NK - Number of temperature-dependent scattering matrices on the library

ID - Identification number of the library

Record type 2 (energy group boundaries and fission spectrum)

This record type specifies the energy group boundaries in eV followed by the fission spectrum. The structure is

(EG(I), I=1, IMP, -1), (XSI(K), K=18, 1, -1)

[c]The term card-image format is used here in the sense that the data are given in a formatted form which can usually be readily exchanged between installations with different computers.

where IMP is IX+1 and IX is the number of MUPO groups. The fission spectrum is given for the 18 fast and epithermal MUPO groups.

Record type 3 (temperature-independent average cross sections)

This record type is used to present the group-averaged cross sections. The data are given successively for NI nuclides. The structure is

(BU(I), I=1, 6), ANU, A, XMU, (DUM, I=10, 21),
(XT(I), I=IX, 1, -1), (XA(I), I=IX, 1, -1),
(XP(I), I=IX, 1, -1), (XF(I), I=IX, 1, -1)

where

BU - Text describing the nuclide

ANU - Type of nuclide

< 0 nuclide is non-fissionable

> 0 nuclide is fissionable

A - Decay constant of the nuclide

XMU - 1-μ_L, where μ_L is the average scattering angle in the laboratory system

DUM - Yields for the 12 most important fission products if ANU > 0, otherwise zeros

(These quantities are not used in a TOTMOS calculation.)

XT - Transport cross section

XA - Absorption cross section

XP - Production cross section

XF - Fission cross section

Record type 4 (mass number, scattering cross section, and mean logarithmic energy loss for moderators)

The structure is

(TXT(I), I=1, 6), MC, SSC, XIC, MBE, SSBE, XIBE, MWA, SSWA, XIWA,
MSW, SSSW, XISW

where

TXT - Text describing the data of this record

MC - Mass number of graphite

SSC - Scattering cross section of graphite

XIC - Mean logarithmic energy loss in graphite

MBE - Mass number of beryllium

SSBE - Scattering cross section of beryllium

XIBE - Mean logarithmic energy loss in beryllium

MWA - Mass number of water

SSWA - Scattering cross section of water

XIWA - Mean logarithmic energy loss in water

MSW - Mass number of heavy water

SSSW - Scattering cross section of heavy water

XISW - Mean logarithmic energy loss in heavy water

Record type 5 (information describing the tables of resonance cross sections)

This record type is used to identify the resonance cross sections for the resonance nuclide K (K = 1, 2, $\cdots$, NJ). The structure is

(X(I), I=1, 9), JRES(K), IEZ(K)

where

X - Text describing the resonance nuclide K

JRES - Identification number of the resonance nuclide

IEZ - Array length of the resonance cross section table

Record type 6 (tables of resonance cross sections)

This record type is used to present tables of resonance cross sections. One table contains the resonance cross sections of a resonance nuclide for a number of temperatures and potential scattering cross sections. The total number of temperatures and potential scattering cross sections must be 25, while the partition between these parameters may be arbitrary. The structure is

(RES(I), I=1, N)

where N is 25*IEZ+1 and RES(1) is the potential scattering cross section for the resonance absorber.

Record type 7 (information on the temperature-dependent scattering matrices)

This record type is used to identify the scattering matrix I (I = 1, 2, $\cdots$, NK). The structure of the record is

(TXT(L), L=1, 9), DI(I), X(I), IEZ(I)

where

TXT - Text describing the scattering matrix

DI - Identification number of the scattering matrix

X - Temperature in Kelvin for which the scattering matrix was calculated

IEZ - Array length of the scattering matrix

Record type 8 (temperature-dependent scattering matrices)

This record type is used to read the temperature-dependent scattering matrix. The structure is

(RES(K), K=1, NL1)

where NL1 = IEZ. The structure of the array RES is as follows:

Magic word for a group

Terms for scattering from the group

Magic word for the next group

Terms for scattering from this group

$\vdots$.

The magic word MW is defined for each source group NKK by

MW = NII - 1 + 0.01*(NJJ -1) + 0.00001*NKK

where NII is the number of the first group into which the group NKK scatters and NJJ is the number of the last group into which the group NKK scatters. The magic word is used in order to suppress the storing of zero values in the scattering matrix, which appear outside the range characterized by the magic word.

9 CELL-WEIGHTED AND "INNER-CELL"-WEIGHTED CROSS SECTIONS

Once the neutron flux has been computed within the reactor cell, the results may be incorporated into the gross diffusion calculations for the whole reactor, in which the detailed structure within the cell is no longer considered. For this purpose, the cross sections of the different nuclides present in the cell are homogenized in order to obtain so-called cell-weighted or "effective" cross sections. The procedure for determining the effective cross sections is based on the requirement that the reaction rates are preserved in the homogenization process, i.e.

$$\bar{\sigma}_G \bar{N} \int_{cell} dV \int_G dE \Phi(\mathbf{r}, E) = \int_{cell} dV N(\mathbf{r}) \int_G dE\, \sigma(\mathbf{r}, E) \Phi(\mathbf{r}, E) \tag{181}$$

where

$\bar{\sigma}_G$ = cell-weighted cross section in group G,

$\sigma(\mathbf{r}, E)$ = space- and energy-dependent cross section,

$N(\mathbf{r})$ = space-dependent atomic number density,

$\Phi(\mathbf{r}, E)$ = space- and energy-dependent weighting function.

Furthermore, $\bar{N}$ is the homogenized atomic number density in the cell, which is given by

$$\bar{N} = \frac{1}{V_{cell}} \int_{cell} dV N(\mathbf{r})\,, \tag{182}$$

where V_{cell} is the total volume of the cell.

The TOTMOS code has been programmed so that it is able to generate two types of weighted cross sections. The first weighting type is the common cell-weighting over the whole cell. This is the usual option to generate cross sections for a gross reactor calculation. The second weighting type is the inner-cell-weighting. In this case, the weighting is performed over specified inner zones of the system under consideration. Which of the inner zones M_1 to M_2 are to be considered in the weighting process can be defined in the TOTMOS input. This option is generally employed as follows. A "cell" is described in the same manner as for the common cell-weighting except that in this case it may be surrounded by a homogeneous representation for the remainder of the core or by a reflector, etc. The flux calculation is then

made for the complete system, by which a more realistic treatment of the leakage across the outer boundary of the interior cell can be made. The cell-weighting is subsequently performed only over the interior cell. If the multigroup notation is used and if the cross sections and the atom number densities are constant within a spatial zone, Eq. (181) becomes

$$\bar{\sigma}_G \, \bar{N} \sum_{j=M_1}^{M_2} \sum_{g \in G} \Phi_{jg} = \sum_{j=M_1}^{M_2} N_j \sum_{g \in G} \sigma_{jg} \Phi_{jg} \, , \tag{183}$$

where

$$\Phi_{jg} = \int_{V_j} dV \int_{E_{g+1}}^{E_g} dE \, \Phi(\mathbf{r}, E) \, . \tag{184}$$

The energy integration in Eq. (184) is to be performed over the fine group g and the spatial integration over the zone j, where V_j denotes in this context the volume of the zone j. Furthermore, it holds that

$$\bar{N} = \frac{1}{V} \sum_{j=M_1}^{M_2} N_j V_j \, . \tag{185}$$

In a similar manner, the group-to-group transfer cross sections are cell-weighted. Here, it is required that the scattering rates from one group to the other are conserved in the cell, i.e.

$$\bar{\sigma}^s_{G' \to G} \bar{N} \int_{cell} dV \int_{G'} dE' \, \Phi(\mathbf{r}, E') = \int_{cell} dV \, N(\mathbf{r}) \int_{G'} dE' \, \Phi(\mathbf{r}, E') \int_G dE \, \sigma_s(\mathbf{r}, E' \to E) \, . \tag{186}$$

If the multigroup notation is used again, the following equation is obtained

$$\bar{\sigma}^s_{G' \to G} \, \bar{N} \sum_{j=M_1}^{M_2} \sum_{g' \in G'} \Phi_{jg'} = \sum_{j=M_1}^{M_2} N_j \sum_{g' \in G'} \Phi_{jg'} \sum_{g \in G} \sigma^s_{j \, g' \to g} \, . \tag{187}$$

The sums over the fine group fluxes on the left side of Eqs.(183) and (187) may be replaced by the broad-group flux $\Phi_{j\,G}$, because

$$\Phi_{j\,G} = \sum_{g \in G} \Phi_{jg} \, . \tag{188}$$

The TOTMOS code calculates both microscopic and macroscopic cell-weighted and condensed cross sections. The microscopic cross sections are written on the external unit IRG3. The data stored are the absorption, fission, production, and transport cross sections. Subsequently the scattering matrices are given. The macroscopic cross sections are processed in

a such form that they can be employed in the CITATION diffusion code.[28] The computed broad-group data are in this case the diffusion constants, the removal cross sections, the fission and production cross sections, and the scattering matrices. The data are written on the external unit 27.

On the basis of the cell-weighted cross section, the TOTMOS code also calculates disadvantage (or shielding) factors which are defined as the ratio of the actual reaction rate and that which would be found for the same material exposed to the volume averaged flux. In the fine-group picture, the disadvantage factors are given by

$$d_g = \frac{\int_{cell} N(\mathbf{r})\sigma_g(\mathbf{r})\Phi_g(\mathbf{r})dV}{\int_{cell} \Phi_g(\mathbf{r})dV \int_{cell} N(\mathbf{r})\sigma_g(\mathbf{r})dV} \,. \tag{189}$$

In terms of d_g, the cell-weighted cross section may be written as

$$\bar{\sigma}_g \bar{N} = d_g \frac{\int_{cell} dV N(\mathbf{r})\, \sigma_g(\mathbf{r})}{V_{cell}} \,. \tag{190}$$

The disadvantage factors are stored on the external unit NSX and are used when the homogenized cross sections for a double heterogeneous system are computed.

10 THE METHOD OF "EQUIVALENT" CROSS SECTIONS

The representation of absorber rods in diffusion calculations for the whole reactor requires special considerations, since the diffusion theory fails within and in the vicinity of strong absorbers. The use of "equivalent" cross sections represents one of the methods which enable the application of a diffusion code for this type of calculations.[2–4] The basis of this method is to determine cross sections for the absorber region on the basis of a transport calculation, which can subsequently be used in the diffusion calculation such that the reaction rates in and the leakage into the absorber region are the same in both types of calculations. The method used in the TOTMOS code for determining equivalent cross sections was developed in connection with the diffusion code CITATION.

It should be mentioned that the method of equivalent cross sections described in this report differs from the original method given in Ref. 2. Although the term of the equivalence is still used here it has a different meaning and is employed only in connection with the determination of the diffusion constant for the absorber rod region. In contrast to the previous method, the equivalence of certain neutron fluxes from the transport and the diffusion calculation is now required in the calculation of the diffusion constant while the cross sections for the absorber rod region correspond those which are obtained in the conventional homogenization by the use of the flux-volume-weighting.

The basic features of the present method are:

- The cylindrical absorber rod is represented in the r-ϕ-z or the x-y-z mesh of the CITATION code by conserving the rod volume.

- The neutron fluxes and reaction rates in the absorber rod and its surroundings are determined by a one-dimensional (1-d) transport calculation in fine energy groups.

- The transport fluxes and the diffusion fluxes at a sufficiently great distance from the surface of the absorber rod are assumed to be equivalent.

- The transport fluxes and the diffusion fluxes in space points having the same distance from the surface or from the center of the rod are assumed to be equivalent independent

of the geometry.

- The numerical procedure used for calculating the leakage in the CITATION code is included in the calculation of the equivalent cross sections.

- The absorber rod is represented in the CITATION calculation by one mesh element in the plane perpendicular to the rod.

The method for determining equivalent cross sections as is described in the following was developed for the x-y-z geometry of the CITATION code. A z-dependence of the absorber rod is not considered in the calculation of the equivalent cross sections so that the explanations are restricted to the x-y plane, in which the absorber rod is represented by a rectangle. If an axial dependence needs to be considered, the absorber rod has to be subdivded into several axial regions and a TOTMOS calculation has to be made for each of these regions. The statements made in the following are also valid for a sector of a circular ring, by which the rod is described in r-ϕ geometry, if the rod is not located too near to the center of the system considered.

In the CITATION calculation, the rectangle of the rod region is surrounded by four neighboring mesh elements. The right and the left mesh elements and the front and back mesh elements shall be identical. The side length of the rod mesh element in the x-direction is denoted in the following by a and the side length in the y-direction by $b = p\,a$. The side length of the neighboring mesh element in the x-direction is denoted by $c = p_x\,a$ and that in the y-direction by $d = p_y\,b = p_y\,p\,a$ (see Fig. 7). When the values of a, p, p_x, p_y are given, the CITATION mesh for the absorber region is fixed. The equivalent rod data can then be determined as a function of these parameters by the use of the principles given above.

If R is the radius of the absorber rod (or of the region to be represented), the volume-true representation of the absorber region in the CITATION calculation requires

$$\pi R^2 = p\,a^2\,. \tag{191}$$

By the use of Eq. (191) either the side length a or the parameter p can be determined. The values of p_x and p_y can be chosen freely and are read in the TOTMOS input.

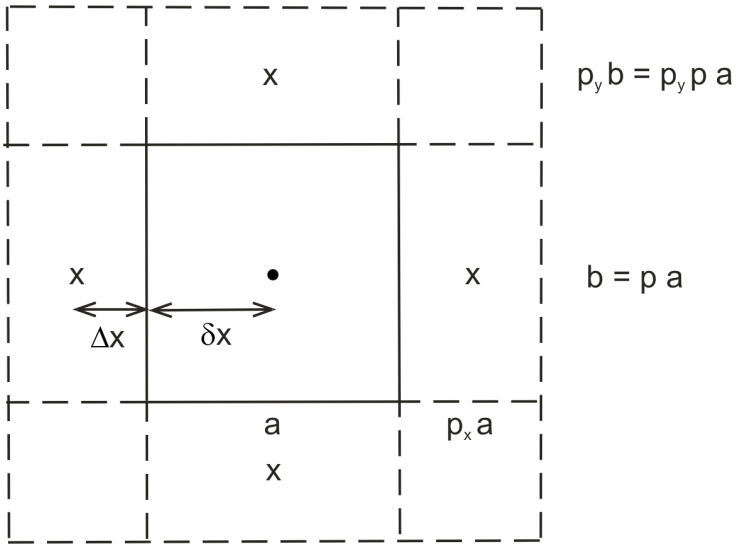

Fig. 7: CITATION mesh for the absorber region.

The 1-d transport calculation for the absorber rod gives the following information which is needed for the determination of the equivalent cross sections:

- the average flux $\bar{\Psi}_R$ in the rod region,

- the homogenized cross sections in the rod region,

- all reaction rates in the rod including the leakage,

- the one-dimensional flux distribution $\Psi_R(r)$ in the vicinity of the absober rod.

The problem is the assignment of the CITATION fluxes in the four neighboring mesh elements of the absorber rod (see Fig. 7) to the transport fluxes in the vicinity of the absorber rod. Since the transport calculation provides no two-dimensional information, a certain arbitrariness in this assigment cannot be avoided. If necessary, a two-dimensional transport calculation may be performed. According to the principles given above, fluxes at points which have the same distance from the surface of the rod (this procedure is denoted in the following as Method I) or from the center of the rod (this procedure is denoted in the following as Method II) are considered to be equivalent. Furthermore, the right and the left

neighboring mesh element of the rod and the front and the back mesh element of the rod are considered as equivalent.

In the CITATION model, the reference point for the flux has the distance

$$\Delta x = \frac{1}{2} p_x \, a \tag{192}$$

from the surface of the rod mesh element in the x-direction. Correspondingly, it holds for the y-direction

$$\Delta y = \frac{1}{2} p_y \, p \, a \, . \tag{193}$$

For Method I, the reference points for the flux in the 1-d transport calculation are thus to be located at the positions

$$R2_x^o = R + \Delta x = a \left(\sqrt{\frac{p}{\pi}} + \frac{1}{2} p_x \right) \tag{194}$$

and

$$R2_y^o = R + \Delta y = a \left(\sqrt{\frac{p}{\pi}} + \frac{1}{2} p \, p_y \right) \, . \tag{195}$$

For Method II, they are to be located at

$$R2_x^c = \frac{1}{2} a (1 + p_x) \tag{196}$$

and

$$R2_y^c = \frac{1}{2} p a (1 + p_y) \, . \tag{197}$$

The transport fluxes at these points are considered to be equivalent to the CITATION fluxes in the neighboring intervals of the absorber rod. Thus, the transport calculation must have interval midpoints at the radii $r = R2_x$ and $r = R2_y$. Which of the two methods for calculating the position of the reference points is more accurate cannot be decided without knowing further details. A sensitivity study may help in a specific case.

For the rod mesh element, the leakage per unit length in the z-direction is calculated in the CITATION code by the relation

$$L_c = \frac{A_y (\Phi_x - \Phi_R)}{\delta_x / D_R + \Delta x / D_s} + \frac{A_x (\Phi_y - \Phi_R)}{\delta_y / D_R + \Delta y / D_s} \, . \tag{198}$$

The quantities used in Eq. (198) have the following meaning:

$\Phi_x = \Phi(x-\text{neighbor})$ and $\Phi_y = \Phi(y-\text{neighbor})$ with

$\Phi_x \equiv \Psi(\mathrm{R2}_x)$ and $\Phi_y \equiv \Psi(\mathrm{R2}_y)$

$\Phi_R = \Phi(\mathrm{rodmeshelement}) \equiv \bar{\Psi}_R$

A_x = area to the y-neighbor $= 2a$

A_y = area to the x-neighbor $= 2pa$

δ_x = distance of the center of the rod mesh element to the x-surface $= \frac{1}{2}a$

δ_y = distance of the center of the rod mesh element to the y-surface $= \frac{1}{2}pa$

D_R = diffusion constant in the rod mesh element

D_s = diffusion constant in the neighboring mesh elements

The effect of the anisotropic diffusion is not considered in the present version of the TOTMOS code.

If the quantities Φ_x, Φ_y, Φ_R, and L_c are set equal to the corresponding values of the transport calculation, the diffusion constant D_R can be determined by the use of Eq. (198). Thus

$$\frac{1}{D_R} = 2p\frac{\Phi_x - \Phi_R}{L} + \frac{2}{p}\frac{\Phi_y - \Phi_R}{L} - \frac{p_x + p_y}{2D_s} + \sqrt{X} \tag{199}$$

where

$$X = \left(2p\frac{\Phi_x - \Phi_R}{L} + \frac{2}{p}\frac{\Phi_y - \Phi_R}{L} + \frac{p_x - p_y}{2D_s}\right)^2 + 4p(p_x - p_y)\frac{\Phi_x - \Phi_R}{L}\frac{1}{D_s} \tag{200}$$

Thus, the homogenized reaction cross sections give the correct reaction rates in the diffusion calculation, and the use of the diffusion constant in Eq. (199) yields the correct leakage term. The region over which the homogenization is made can again be specified by the parameters M_1 and M_2, which are defined in the TOTMOS input (see also Section 9).

The method described above to calculate the equivalent cross sections can be also employed to treat a central absorber rod in r-z cylinder geometry. For this purpose the geometric dimensions defined in the input for the x-y mesh are converted into the corresponding dimensions as are required for the r-z geometry. If a triangular mesh is used in the CITATION calculation the method can be furthermore applied to determine the equivalent cross sections for a symmetric triangular absorber rod. A description of the spatial parameters defining the triangular mesh is given in the CITATION report.

It should be mentioned here that the TOTMOS code additionally calculates "equivalent", i.e. the CITATION mesh adapted, rod constants.[3] Within the frame of the diffusion theory,

the leakage into the absorber region may be written in the form[15]

$$L = A_R \, \Phi_R \, C_R \,, \tag{201}$$

where the rod constant C_R is defined by

$$C_R = - \left. \frac{D_s}{\Phi_R} \frac{\partial \Phi(r)}{\partial r} \right|_{r=R} \tag{202}$$

The radius R defines the rod boundary and A_R is the surface of the absorber. The relation in Eq. (202) is used in the CITATION code in the form of a boundary condition and its use is explained in more detail in the CITATION report. Using this method the restriction that the absorber rod region has to be represented by one mesh element in the CITATION calculation is no longer necessary. A drawback of the method, however, is that only one rod constant C_R can be defined for all absorber rod regions in the CITATION calculation.

The rod constant C_R is usually determined by the relation

$$C_R = \left. \frac{j(r)}{\Phi(r)} \right|_{r=R} \tag{203}$$

where $j(R)$ is the net current at the boundary of the absorber region. The ratio of the net current density to the flux may be computed by a transport calculation for the absorber rod and the resulting value of C_R may be used in a subsequent CITATION calculation in which the leakage into the absorber region is determined by the equation

$$L_c = \frac{A_y \Phi_x}{1/C_R + \Delta x/D_s} + \frac{A_x \Phi_y}{1/C_R + \Delta y/D_s} \,. \tag{204}$$

The concept developed for the determination of the equivalent cross sections can now also be applied in order to compute the rod constant C_R by the use of Eq. (204). Thus

$$\frac{1}{aC_R} = \frac{\Phi_y + p\Phi_x}{L} - \frac{p_x + pp_y}{4D_s} + \sqrt{Y} \,, \tag{205}$$

where

$$Y = \left(\frac{\Phi_y + p\Phi_x}{L} + \frac{p_x - pp_y}{4D_s} \right)^2 - p(p_x - pp_y) \frac{\Phi_x}{L} \frac{1}{D_s} \,. \tag{206}$$

This procedure for determining the rod constant explicitly considers the method of calculating the leakage in the CITATION code and thus is a methodological improvement compared to the previous procedure. If the method of the equivalent rod constant is employed for determining the efficiency of absorber rods, the restriction to represent an absorber rod by one mesh element is furthermore no longer necessary.

11 DESCRIPTION OF THE TOTMOS SUBROUTINES

The MAIN program defines the length, NLIM, of the array A(NLIM) which contains all the data fields used in a TOTMOS run. The variable NLIM has to be increased if the number of storage allocations for a specific problem is not sufficient.

Subroutine CALLER starts all subroutines, which initiate a new problem area processed in the TOTMOS code. The unit NTLIB is connected to the MUPO cross section library and the unit NTSCR is connected to a scratch device which is used to store the microscopic scattering matrices temporarily. Furthermore, the external units NTPUN and NSX are defined, which are used to store the equivalent cross sections and the disadvantage factors, respectively, computed in a TOTMOS calculation. If the memory allocated in the MAIN program is not sufficient for the problem under consideration, a message is written out and the run is terminated.

Subroutine DIMENS calculates the addresses of all arrays used in a TOTMOS run and determines the total number of allocations required for the problem to be analyzed. The addresses are given in the common KEYS, which are made available in this way to the subroutine CALLER.

For each zone in the system considered, subroutine GEOM successively reads the zone number, the thickness of the zone and the number of spatial intervals in the zone. Using this information the inner and outer radii of the zones, the interval boundaries, and the volumes of the intervals, as well as the total number of intervals, are calculated for the geometry used in the actual TOTMOS run.

Subroutine READNC reads the concentrations of all nuclides considered in the problem to be analyzed. If a double-heterogeneous problem is treated, READNC furthermore reads the zone numbers for the disadvantage factors which have been determined in the first run of the double-heterogeneous calculation and which are used to correct the cross sections to be employed in the second run (see also the input description of the TOTMOS code in Section 12). The disadvantage factors are read from the scratch device NSX and are used in the subroutines MACRO and EDIT1.

Subroutine MUPLIB reads the tabulated multigroup cross section data from the external unit NTLIB. After the general parameters describing the library, the absorption, transport, fission and production cross sections are read. The scattering cross sections required in the TOTMOS calculation are determined from the transport cross sections and the average cosines of the scattering angle in the laboratory system. Subsequently, the resonance cross section tables are read for all temperatures and all potential scattering cross sections given on the library. The resonance cross sections are interpolated at the average fuel temperature in the reactor cell and at the required potential scattering cross section. Furthermore, the scattering matrices of the moderator materials are read for the given temperatures. The data are interpolated in order to determine the scattering matrices at the average moderator temperature in the cell. If required, the subroutine FREEGAS is called, which calculates the scattering matrices of further nuclides in the system on the basis of the free-gas model.

In order to solve the transport equation by an iteration procedure, a starting flux is needed with which the initial fission source is calculated. On request, subroutine WEST determines the different constants required to calculate the initial flux on the basis of the Westcott formalism. The Westcott flux is also used as a weighting function in order to determine the group-to-group transfer cross sections when these are computed on the basis of the free-gas scattering model.

Subroutine FREEGAS calculates the thermal scattering kernels of the free-gas model by the Brown and St. John formalism. The thermal scattering kernels are averaged by the Westcott flux in order to compute the thermal group-to-group transfer cross sections of the free-gas model. The group-to-group transfer cross sections in the fast energy range are calculated on the assumption that the scatterers are at rest and that the scattering is isotropic in the center-of-mass system.

For some nuclides, as for example the fissionable nuclides or the fission products, it is not necessary to consider for the complete scattering matrix in the transport calculation. For these nuclides no scattering matrices are given on the MUPO library. Instead, subroutine DIAG generates an artificial scattering matrix for these nuclides, which contains the total scattering cross section at the position of the self-scatter term of the scattering matrix. The other elements of the scattering matrix are set equal to zero. This procedure saves computer

memory and guarantees that the particle balances is fulfilled.

Subroutine OUTNC prints the mixing table, which instructs which nuclide is to be added to the different material mixtures in which concentration.

Subroutine MACRO calculates the required macroscopic cross sections by the use of the nuclide concentrations read in subroutine READNC. These are the macroscopic absorption, fission and production cross sections. Furthermore, the macroscopic scattering matrices are determined. The total cross section is calculated as the sum of the absorption and the scattering cross section. If the calculation to be made is the second run of a double-heterogeneous calculation, the self-shielding factors, determined in the first run and read in subroutine READNC from the external unit NSX, are taken into account in the computation of the macroscopic cross sections to be used in the second run. If requested, the macroscopic cross sections are printed out.

Subroutine TRANSK calculates the escape probabilities, the collision probabilities, and the transport coefficients for the spatial mesh defined by subroutine GEOM and by the use of the total cross sections determined in subroutine MACRO. A buckling correction may be made in order to consider an axial leakage. The required buckling values are defined in the TOTMOS input. They are assumed to be spatially constant and can be group-dependent. The buckling data may be read in the form of DB^2 or B^2 values. If they are read as B^2 values, a fine group diffusion constant D is determined by the use of the total cross section with which the quantity DB^2 is computed. In the case of an albedo boundary condition the albedo values are read by group. Subsequently, the geometrical and optical path lengths of the possible flight paths in the individual intervals of the reactor cell are determined. The escape probabilities and the collision probabilities are then calculated for the outgoing directions. The collision probabilities for the incoming directions are determined by applying the reciprocity relation for the collision probabilities. In order to guarantee that the particle balance is not detrimentally influenced by numerical inaccuracies, the collision probabilities and the escape probabilities for leaving the whole system are normalized. Controlled by an input option, the escape probabilities, the collision probabilities and the normalization factors may be printed out. If an albedo or white boundary condition is used, the collision probabilities are corrected for this effect using the albedo values given in the input. Finally, the transport

coefficients are calculated by using the relation between the transport coefficients and the collision probabilities. The transport coefficients may be printed out on request.

The functions F1, F2, and F3 calculate the values of the Bickley functions Ki_1, Ki_2, and Ki_3 for a given argument in the case of cylindrical geometry. For spherical geometry, the value of the exponential function is determined. The functions are called by subroutine TRANSK.

The numerical solution of the integral transport equation is carried out in subroutine FLUX. First, the initial fission source is calculated by the use of a flux estimate. The fluxes may be energy-dependent and are assumed to be constant over the system considered. The starting fluxes are either determined on the basis of the Westcott formalism or are read in the input. The fission source is normalized to unity and the initial fluxes are normalized such that the total losses in the system are unity. The normalized fluxes are then used for the calculation of the initial scattering source. The new spatial distribution of the neutron flux within a single energy group is calculated by the power iteration method, which is accelerated by additional iteration techniques. These are renormalization, over-relaxation, and extrapolation, which is a special form of over-relaxation. After a complete run through all energy groups, which corresponds to a source (or an outer) iteration, the new fluxes are renormalized such that the total losses in the system are unity (global scaling). Furthermore, new values for the mean squared residuals (see Section 6) are determined. Subsequently, subroutine RELAX is called, which calculates the over-relaxation factors. The new fluxes are extrapolated or over-corrected, if the conditions which are defined in the code by default values or in the input are fulfilled for these corrections. The scattering source is recalculated with the new fluxes and the power iterations are started again. If the relative deviations of the fluxes in two subsequent iterations are smaller than a predetermined value, the power iterations are terminated. The fission source is then recalculated with the new fluxes. Furthermore, a new eigenvalue is determined, which is used to correct the fission source in order to keep the number of neutrons in the system nearly constant from one outer iteration to the next. The new fission source is again normalized to unity. Subsequently, the power iterations are started again and new fluxes are calculated by the use of the new fission source. If the deviations of the fission sources in two subsequent outer iterations are smaller than a given

value, the outer iterations are converged and the iteration process is terminated. At the end, the converged fluxes are normalized again such that the total losses in the system are unity and thus equal to the fission source.

In a first call, subroutine RELAX assigns default values to the iteration parameters, which may be overwritten by values defined in the input. During the power iterations, subroutine RELAX is called in order to calculate appropriate over-relexation factors for accelerating the iterations. If the over-relaxation factors for the extrapolation are equal within a given limit and in a predetermined number of subsequent iterations, an extrapolation of the fluxes is performed. Furthermore, an optimum over-relaxation factor is sought in order to refine the extrapolated solution in the subsequent iterations. An iteration monitor edits the iteration number at which the extrapolation is made, the extrapolation factor, the lowest μ eigenvalue, the lowest λ eigenvalue and the present value of the optimum over-relaxation factor (see Section 6).

Subroutine EDIT lists the neutron fluxes in the zones of the system considered in three different ways. The group fluxes in the zone (integrated fluxes) are edited as are the zone averaged group fluxes (group fluxes), and the zone and group-averaged fluxes (averaged fluxes). Furthermore, disadvantage factors by group are edited for each zone. The above data are also given for the total system. In addition, subroutine EDIT calculates and prints balance tables for all zones and for the total system. The balance tables contain the absorption rate, the fission source, the fission rate, the inscatter and outscatter rate, the total scattering rate and the total collision rate. Furthermore, the radial leakage out of the system and the leakage due to axial buckling are determined and listed. Further data of a TOTMOS calculation are written on the external unit NFLU1 for later processing. These are the title card, the number of energy groups and the number of intervals used in the problem. Furthermore, the widths of the energy groups and the midpoints of the energy groups are written. For each interval, the midpoint of the interval and the scalar neutron fluxes per lethargy unit in the interval are subsequently stored for all energy groups. Subsequently, subroutine EDIT1 is called for computing the homogenized cross sections. If required, subroutine RCS is called in order to determine the equivalent cross sections. Finally, the fine-group disadvantage factors are written for all zones on the external unit NSX.

Subroutine EDIT1 calculates the cell-weighted and condensed cross sections. The nuclides, for which the weighted cross sections are determined, may be defined in the input. Otherwise the data of all nuclides used in the problem under consideration are weighted and condensed. An additional input option allows the zones to be specified over which the cross sections are weighted. Both microscopic and macroscopic cell-weighted cross sections are calculated. The macroscopic data are written on an external unit in a such form that they can be read by the CITATION code in order to be employed in a subsequent diffusion calculation for the gross reactor. The weighted microscopic cross sections are stored on the external unit IRG3. If the calculation performed is the second run of a double-heterogeneous calculation, the self-shielding factors determined in the first run are taken into account in the computation of the macroscopic cell-weighted cross sections.

For those zones for which the cell-weighting has been performed, subroutine EDIT2 lists the broad-group fluxes in the zone, the zone-averaged broad-group fluxes, and the zone- and broad-group-averaged fluxes, as well as the broad-group disadvantage factors. These quantities are also given for the whole system.

Subroutine RCS provides the equivalent cross sections, which may be employed in absorber rod calculations for the gross reactor by the use of the diffusion code CITATION. The macroscopic cell-weighted cross sections for the absorber cell computed in the subroutine EDIT1 are made available to RCS via the parameter list. At the beginning, the RCS routine reads the parameters which define the mesh for the absorber rod and its surroundings as is used in the CITATION code (see also the explanations in Section 9). Furthermore, the broad-group diffusion constants for the surroundings of the absorber rod are read. Subsequently, the numbers of the zones containing the reference points for the fluxes in the TOTMOS transport calculation are defined via the input. By the use of the transport fluxes in the reference points, the geometric parameters for the CITATION mesh, and the diffusion constants of the absorber surroundings, the leakage into the absorber rod is employed in order to determine the group-dependent diffusion constants for the absorber region. The diffusion constants thus determined and the cell-weighted cross sections are written on the external unit NTPUN in such a format that the data can be directly used in a subsequent CITATION calculation. The method of equivalent cross section can also be applied if a sym-

metric triangular mesh is used in the CITATION calculation. In addition to the equivalent cross sections, the subroutine RCS computes equivalent rod constants, which may also be employed in absorber rod calculations for the gross reactor by the use of a diffusion code.

12 INPUT INSTRUCTIONS

The input data required to run a problem using the TOTMOS code are given in the following. Each section of input data is itemized and provided with a short comment. The input format with which the data are read is given in parentheses. Some input arrays or some blocks of data are only required if a related integer variable read in before exhibits a specific value. The condition whether such an array needs to be read is given in braces. The number of entries in each array is denoted in square brackets. In order to facilitate the input, some default values have been programmed into the TOTMOS code. Where such values exist, they are given in parentheses.

12.1 Input Data

A) Title Card (a72)

B) General Parameters (14i5)

1. IX - Number of energy groups
2. NX - Number of spatial intervals
3. MX - Number of zones
4. NNUC - Number of nuclides considered in the problem
5. NRES - Number of resonance nuclides
6. NSTREU - Number of nuclides with scattering matrices
7. NGAS - Number of nuclides with free-gas kernel computation
8. MSUB - Number of subgroups per thermal group in the computation of the group-to-group transfer matrix of the free-gas model (2)
9. INF - Editing options

   0 - no effect

   ≥ 1 - print one-dimensional macroscopic cross sections

   ≥ 2 - print energy group boundaries, energy midpoints, group widths, and macroscopic scattering matrices

   ≥ 3 - print transport coefficients and non-leakage probabilities

≥ 4 - print escape and collision probabilities

10. NXOLD - option for a double heterogeneous calculation (DHC)

    ≤ 0 - simple heterogeneous calculation or first run of a DHC

    (It is set in the code MXOLD = 1.)

    > 0 - number of zones in the first run of a DHC

    (It is set in the code MXOLD = NXOLD.)

11. NBURN - option for boron-10 burn-up calculation

    ≤ 0 - no effect

    > 0 - burn-up calculation with NBURN time steps

C) Parameters Defining the Burn-up Calculation {NBURN > 0} (5x, i5, 2e15.5)

1. MREF - Number of the zone which is used as a reference zone for the determination of the flux level
2. FREF - Average group flux (cm^{-2} s^{-1}) in zone MREF
3. DELTAT - Time interval (days) for the burn-up calculation

D) Geometry Data (14i5)

1. NGEOM - Problem Geometry

   0 - cylinder

   1 - sphere

E) Definition of the Material Zones and Spatial Intervals (2i5, e10.4)

1. NR - Zone number in ascending order
2. NP - Number of intervals in the zone
3. TH - Thickness of the zone

Repeat card E for all zones in the reactor cell and terminate the geometry input by a blank card.

F) Information on the Cross Section Data of the Nuclides Used in the Calculation (2i5, 6e10.4)

1. KDNUC - Nuclide identification number
2. KSTREU - Option for the treatment of the scattering matrix

   -1 - calculate scattering matrix by the use of the free-gas model

   0 - scattering matrix contains only self-scatter term (for strong absorber only)

1 - read scattering matrix from the MUPO cross section library (BeO, C, H_2O, and D_2O)

3. AAM - Mass number of the nuclide
4. APPA - κ value used in the resonance calculation (only for Th-232, U-238, Pu-240, and Pu-242)

G) Free-Gas Kernel Calculation (i5, 5x, 6e10.4 and, if required, 7e10.4) {KSTREU = -1}

1. KG - Number of summands in the free-gas kernel representation ($0 < KG < 6$), (AKAP(I), BKAP(I), I = 1, KG) - Exponents and pre-factors in the series expansion of the free-gas scattering cross section

H) Contribution of the Nuclide KDNUC to the Material Mixtures

1. DEN - Nuclide concentration by zone [MX] (7e10.4)

I) Data Required in the Second Run of a DHC {MXOLD > 1}

1. MDF - Numbers of the zones in which nuclide KDNUC appears in the first run of a DHC. The possible values are 1 to MXOLD and are used for the assignment of the disadvantage factors determined in the first run [MX] (7i10)

Repeat cards F to I for each nuclide required and terminate this part of the input by a blank card.

J) Material Temperatures

1. TEMP1 - Fuel temperatures in Kelvin by zone [MX] (7e10.4)
2. TEMP2 - Moderator temperatures in Kelvin by zone [MX] (7e10.4)

K) Boundary Condition and Buckling Data (2i5, e10.4)

1. LEAKT - Boundary condition at the right boundary of the system

   -1 - albedo boundary

   0 - vacuum boundary

   1 - white boundary

2. NBUC - Option for buckling correction

   -1 - B^2 values by group

   0 - no effect

   1 - DB^2 values by group

3. WEGMIN - Parameter in the transport kernel calculation (10^{-4})

L) Buckling Values {|NBUC| $\neq 0$} 5(i5, e10.0)

1. (IG(I), DBSQ(I), I = 1, 5) - Limit group, B^2 or DB^2 values for the groups IG(I-1)+1 to IG(I), where IG(0) = 0

M) Albedo Values {LEAKT < 0} 5(i5, e10.0)

1. (IG(I), ALBEDO(I), I = 1, 5) - Limit group, albedo values for the groups IG(I-1)+1 to IG(I), where IG(0) = 0

N) Iteration Parameters (each value can be individually overwritten) (4i5, 6e10.4)

1. ITMAX - Flux iteration maximum (100)
2. ITBG - Minimum iterations before extrapolation (20)
3. LCMX - Number of over-relaxation factors tested (6)
4. ITDM - Minimum delay between extrapolations (10)
5. EPS - Scalar flux convergence criterion (10^{-4})
6. RELC - Initial over-relaxation factor (1.9)
7. EPSG - Extrapolation criterion (0.05)
8. OVERX - Maximum extrapolation factor (100)
9. FACTOR - Under-extrapolation factor (1.0)

O) Parameters for the Starting Flux and the Source Iterations (2i5, e10.4)

1. IFLUX - Option for the flux guess

   0 - Westcott flux (calculated in TOTMOS)

   > 0 - input flux guess
2. ITA - Number of outer iterations (50)
3. EPSK - Convergence criterion for the source iterations (10^{-5})

P) Flux Guess {IFLUX > 0}

1. F - Flux values by group [IX] (7e10.4)

   The fluxes are used in each interval of the system considered.

Q) Parameters for the Cross Section Condensation and Homogenization (14i5)

1. NBRGR - Number of broad energy groups
2. NDUM - Not used
3. NCD - Option for the condensation

   0 - this is the last condensation

1 - a further condensation is made

-1 - module RCS is called in this condensation in order to calculate equivalent cross sections for absorber rods

4. MM1 - Innermost zone in the spatial homogenization
5. MM2 - Outermost zone in the spatial homogenization
6. MNNUC - Number of nuclides for which broad-group and homogenized cross sections are generated. If MNNUC = 0, the data of all nuclides used in this calculation are condensed and homogenized.

R) Nuclides for which Condensed and Homogenized Cross Sections are to be Generated {MNNUC > 0}

1. INUC - Nuclide identification numbers [MNNUC] (14i5)

S) Definition of the Broad Groups

1. LIM - Broad groups specified by fine group numbers [NBRGR] (35i2)

Repeat the cards Q to S for all condensation and homogenization procedures required and set NCD = 0 in card Q in the last condensation and homogenization.

T) Data Required in the Calculation of the Equivalent Cross Sections {NCD = -1}

1. TITLE - Title card (TITLE(1) is the number of the CITATION zone in which the equivalent cross sections are used.) (15a4)

U) General Parameters {NCD = -1} (5i5)

1. IGEOM - Geometry of the Absorber

   1 - slab

   2 - cylinder

   3 - sphere

2. ITYP - Specification of the Absorber

   1 - central rod

   2 - symmetric triangular rod

   3 - excentric rod

3. METH - Method for Calculating the Flux Reference Points

   1 - reference point R2S is counted from the outer boundary

   2 - reference point R2S is counted from the center of the rod

4. MKX - Zone number of the x-reference flux point
5. MKY - Zone number of the y-reference flux point

   The zones MKX and MKY must contain only one mesh element.

V) Information on the Absorber Rod Geometry in CITATION {NCD = -1} (6e12.4)

1. P - Side ratio b/a of the absorber mesh element in CITATION (1.0)
2. PX - Side ratio ax/a of the x-neighbor mesh element in CITATION (1.0)
3. PY - Side ratio by/b of the y-neighbor mesh element in CITATION (1.0)
4. PPX - Relative distance of the reference point from the x-boundary of the absorber mesh element (1.0)
5. PPY - Relative distance of the reference point from the y-boundary of the absorber mesh element (1.0)

   The quantities PPX and PPY are used in special cases, as for example, if the absorber can only be represented by more than one mesh element in CITATION or if the absorber mesh element is a boundary interval.

   (Example: absorber at the x-boundary: $\Rightarrow$ PPX = 0.5)

The detailed description of the CITATION mesh for the absorber rod region is given in Section 10.

W) Diffusion Coefficients in the Region Surrounding the Absorber {NCD = -1}

1. DA - Diffusion coefficients [NBRGR] (6e12.4)

   The diffusion coefficients may be taken from a reactor design calculation.

The second run in a double heterogeneous calculation requires a complete input once again.

12.2 TOTMOS Input/Output Specifications

TOTMOS requires the following input/output assigments

Logical No.	Purpose
NTIN(5)	card input
NTOUT(6)	standard output
NFLU1(2)	device for the external flux storage
NTPUN(7)	library of the equivalent cross sections produced by the TOTMOS code

NTSCR(8)	scratch device
NSX(9)	device for the storage of the disadvantage factors
IRG3(11)	microscopic cell-weighted cross section library produced by the TOTMOS code
NTLIB(17)	MUPO cross section library (input)
27	macroscopic cell-weighted cross section library produced by the TOTMOS code

REFERENCES

1. D. Emendörfer and K. H. Höcker, "Theorie der Kernreaktoren," Part 1, Bibliographisches Institut (1969).

2. W. Scherer and H. J. Neef, "Determination of Equivalent Cross Sections for Representation of Control Rod Regions in Diffusion Calculations," Jül-1311, Kernforschungsanlage Jülich (1976).

3. W. Scherer, "Zur Darstellung von Absorberstäben in Kugelhaufenreaktoren," Internal Report KFA-IRE-IB-21/80, Kernforschungsanlage Jülich (1980).

4. V. Fen, M. Lebedev, V. Sarytchev, and W. Scherer, "Modelling of Neutron Absorbers in High Temperature Reactors by Combined Transport-Diffusion Methods," Forschungszentrum Jülich (1992).

5. H. Honeck, "THERMOS, A Thermalization Transport Theory Code for Reactor Lattice Calculations," BNL-5826, Brookhaven National Laboratory (1961).

6. H. Bonka, "Entwicklung eines Spektralprogramms für kugelförmige Brennelemente sowie Untersuchungen über die Größe und Beeinflussbarkeit des Moderatorkoeffizienten bei Hochtemperaturreaktoren," Jül-746-RG, Kernforschungsanlage Jülich (1971).

7. H. J. Neef, "Berechnung der Wirksamkeit von Absorberstäben in Hochtemperaturreaktoren unter Verwendung transporttheoretisch bestimmter Randbedingungen mit einem dreidimensionalen Diffusionsprogramm," Jül-980-RG, Kernforschungsanlage Jülich (1973).

8. H. J. Neef and W. Scherer, "THERMOS-JÜL, Modifikationen und Korrekturen am thermischen Zellprogramm THERMOS," Internal Report KFA-IRE-IB-26/72, Kernforschungsanlage Jülich (1972).

9. C. L. Bennet and W. L. Purcell, "BRT-I: Batelle Revised THERMOS," BNWL-1434, Batelle-Pacific Northwest Laboratories (1970).

10. H. Gerwin and W. Scherer, unpublished.

11. W. Scherer, unpublished.

12. K. Kugeler and R. Schulten, "Hochtemperaturreaktortechnik", Springer Verlag (1989).

13. W. Scherer, Personal communication.

14. J. Schlösser, "MUPO, An IBM-7090 Programme to Calculate Neutron Spectra and Multi-Group Constants," D.P. Report 172 (1963).

15. H. D. Brown and D. St. John, "Neutron Energy Spectrum in D_2O," DP-33 (1954).

16. C. H. Westcott, W. H. Walker, and T. K. Alexander, *Proc. Second U.N. Conf. on Peaceful Uses of At. Energy*, **16**, 70 (1958).

17. K. M. Case and P. F. Zweifel, "Neutron Transport Theory," Addison-Wesley Publishing Co., Inc. (1967).

18. M. Abramowitz and I. A. Stegun, eds., "Handbook of Mathematical Functions with Formulars, Graphs, and Mathematical Tables," John Wiley and Sons, Inc. (1972).

19. D. Young, *Amer. Math. Soc.* **76**, 92 (1954).

20. R. B. Kellogg and L. C. Noderer, *J. Soc. Indust. Appl. Math.* **8**, No. 4, 654 (1960).

21. K. F. Hansen, "An Exponential Extrapolation Method for Iterative Procedures," ScD Thesis, Mass. Inst. Tech (1958).

22. K. Nünighoff, J. Li, C. Druska, and H.-J. Allelein, Proc. of PHYSOR 2010 - Advances in Reactor Physics to Power the Nuclear Renaissance, Pittsburgh, Pennsylvania (2010).

23. M. Herman, ed., "ENDF-102, ENDF-6 Data Formats and Procedures for the Evaluated Nuclear Data File ENDF-VII," BNL-NCS-44945-01/04-Rev. Brookhaven National Laboratory (2005).

24. R. E. MacFarlane and D. W. Muir: "The NJOY Nuclear Data Processing System," Version 91, LANL-12740-M, Los Alamos National Laboratory (1994).

25. E. Teuchert and R. Breitbarth, "Resonanzintegralberechnung für mehrfach heterogene Anordnungen," Jül-551-RG, Kernforschungsanlage Jülich (1968).

26. L. W. Nordheim and G. F. Kuncir, "A Program of Research and Calculations of Resonance Absorption," GA-2527, General Atomics (1961).

27. J. F. Briesmeister, ed., "MCNP^{TM} - A General Monte Carlo N-Particle Transport Code," Version 4C, LA-13709-M, Los Alamos National Laboratory (2000).

28. T. B. Fowler, D. R. Vondy, and G. W. Cunningham, "Nuclear Reactor Core Analysis Code: CITATION," ORNL-TM-2496, Rev.2, Oak Ridge National Laboratory (1971).

Jül-4325
Juni 2010
ISSN 0944-2952